INTERNATIONAL INSTITUTE OF WELDING

A world of joining experience

German Delegation

IIW-Doc. XIII-2240r1-08/XV-1289r1-08

IIW Guideline for the Fatigue Assessment by Notch Stress Analysis for Welded Structures

Wolfgang Fricke

Hamburg University of Technology
Ship Structural Design and Analysis

May, 2009

Abstract

The notch stress approach for fatigue assessment of welded joints is based on the highest elastic stress at the weld toe or root. In order to avoid arbitrary or infinite stress results, a rounded shape with a reference radius instead of the actual sharp toe or root is usually assumed. Different proposals for reference radii exist, e.g. by Radaj who proposed a fictitious radius of 1 mm to consider micro-structural support effects for steel. The present guideline reviews different proposals for reference radii together with associated S-N curves. Detailed recommendations are given for the numerical analysis of the notch stress by the finite or boundary element method. Several aspects are discussed, such as the structural weakening by keyhole-shaped notches and the consideration of multiaxial stress states. Regarding the fatigue strength, appropriate S-N curves are presented for different materials. Finally, four examples illustrate the application of the approach as well as the variety of structures which can the analysed and the scatter of results obtained from different models.

Keywords: notch stress, fatigue strength, welded joint, notch radius, FEM

1. Introduction

Welded joints are frequently assessed with respect to fatigue by the *S-N curve approach*, using S-N curves (also referred to as Wőhler curves) giving the design fatigue life for constant amplitude loading and an appropriate damage accumulation rule to consider the effect of variable-amplitude loading. The approach may be based on different types of stress at the critical welded joint, i. e.:

- *nominal stress approach*, based on the stress that excludes any stress increase due to the structural detail or the weld
- *structural hot-spot stress* and other structural stress approaches, based on the stress containing only the stress increase due to the structure, but not due to the local weld geometry (usually refers to the weld toe)
- *notch stress approach*, based on the local stress at the weld toe or the weld root, assuming ideal-elastic material behaviour and micro-structural support effects to a certain extent
- *notch stress intensity approach*, using the notch stress intensity factor (NSIF) at the weld toe with zero radius as the fatigue parameter

The approaches use fracture of a specimen or structure as failure criterion. Alternatively, the *elastic-plastic notch strain approach* may be applied, which is based on crack initiation in the material and considers the plasticity effect on fatigue using relevant material properties. Additionally the *crack propagation approach* is applied for computing fatigue lives up to a defined crack length. The crack propagation approach based on fracture mechanics principles is in widespread use as an alternative to the S-N curve approaches, assuming a fictitious or actual initial crack. The approaches have been described in various references, more recently to various degrees by Hobbacher (2007), Niemi et al. (2006), and Radaj et al. (2006), showing their details, potentials and limits.

In comparison with the other approaches, the *notch stress approach* allows the effect of the local weld geometry to be included directly in the stress so that different geometrical configurations can be compared with each other and can even be optimised. Also, the so-called thickness effect is implicitly considered, at least from the geometrical point of view.

As with all local approaches, experience is needed to apply the notch stress approach correctly, to consider its limits and shortcomings and to draw reasonable conclusions from the results. This guideline is intended to help in this respect. First the background of the approach, as outlined by Radaj et al. (2006) and by further, more recent, publications, is summarized, with focus on the numerical methods. Guidelines are then given for the numerical stress analysis and the fatigue classes or design S-N curves used in the fatigue strength assessment. Finally, some examples of practical applications that were analysed in a round-robin are described. One example includes the application of selected approximation formulae for notch stress concentration factors which are still sometimes applied, although the steadily improving numerical methods make direct analyses easier.

The present guideline supplements the fatigue design recommendations of the International Institute of Welding (IIW), which have recently been updated (Hobbacher, 2007). Additional hints and more recent findings are given regarding the notch stress approach, which is applied to an increasing extent, but is still under development. The reader should keep this in mind when applying this approach. Furthermore it is strongly recommended to make comparisons with the other approaches mentioned and to question any differences critically. In this way, the notch stress approach can be expected to contribute to a rational fatigue assessment and to help in the design of sound, fatigue-resistant welded structures.

2. Background of the Approach

2.1 Overview

The notch stress approach considers the increase in local stress at the notch formed by the weld toe or the weld root, based on theory of elasticity, i. e. without consideration of elastic-plastic material behaviour. The micro-structural support effect of the material, which considers the effect on fatigue behaviour of the inhomogeneous material structure under a stress gradient,, can be taken into account by different hypotheses in the (elastic) notch stress approach:

- the *stress gradient approach* (Siebel and Stieler, 1955)
- the *stress averaging approach*, proposed by Neuber (Neuber, 1937, 1946 and 1968)
- The *critical distance approach* (Peterson, 1959)
- the *highly stressed volume approach* (Kuguel, 1961; Sonsino,1994 and 1995).

Only the last three hypotheses have found wide application to welded joints. The stress averaging approach is mainly used in the form of fictitious notch rounding, Fig. 2.1, known also as *effective notch stress approach*, while the critical distance approach employs the ratio of a material constant and the notch radius to reduce the elastic stress concentration factor K_t to the *fatigue notch factor* K_f.

In the following sections, approaches using fictitious notch rounding are described in more detail.

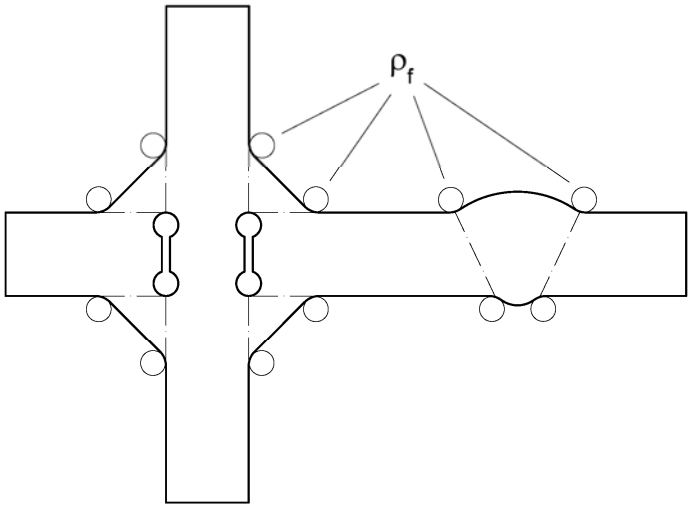

Fig. 2.1: Fictitious notch rounding (graph according to Hobbacher, 1996)

2.2 Notch Rounding Approach

The basic idea behind this approach is that the stress reduction in a notch due to averaging the stress over a certain depth can alternatively be achieved by a fictitious enlargement of the notch radius. Neuber (1968) proposed the following formula for the fictitious radius ρ_f:

$$\rho_f = \rho + s \cdot \rho^* \qquad (2.1)$$

where ρ = actual notch radius
s = factor for stress multiaxiality and strength criterion
ρ^* = substitute micro-structural length

In the approach proposed by Radaj (1990) for welded joints, the factor *s* is assumed to be 2.5 for plane strain conditions at the roots of sharp notches, combined with the von Mises multiaxial strength criterion for ductile materials. Values for the substitute micro-structural length ρ^* for various materials are given in Fig. 2.2. Considering typical welds in (low strength) steel, the choice of ρ^* = 0.4 mm (for cast steel in the welded zone) is appropriate. Both factors result in an increase of the actual radius by 1 mm to obtain the fictitious radius ρ_f according to eq. (2.1). The rounding is applied to both the weld toe and the weld root.

In a 'worst case' or conservative way, Radaj's approach is applied assuming an actual radius of zero so that the fictitious radius, now considered as the *reference radius*, is r_{ref} = 1 mm, see Fig. 2.1. As the stress analysis results in the fatigue-effective stress, the approach is also called *effective notch stress approach*. S-N curves related to the reference radius $r_{1.0}$ are discussed in Section 4.

Attempts have been made to derive a corresponding fictitious radius for aluminium alloys, which would be expected to be much smaller than that for steels assuming the substitute micro-structural length according to Fig. 2.2 (Sonsino et al., 1999). However, more recent investigations have shown that within a rough approximation the same reference radius as for welded joints in steel can also be used for welded joints in aluminium alloys (Morgenstern et al., 2004).

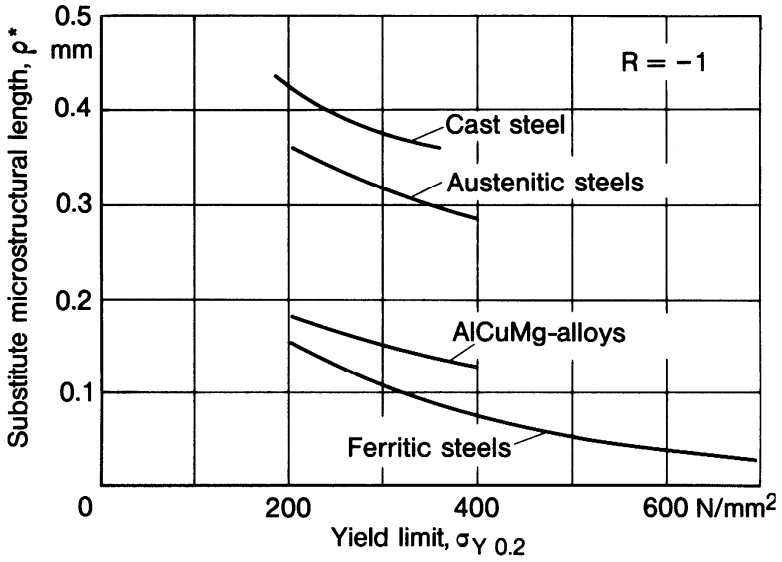

Fig. 2.2: Substitute micro-structural length dependent on yield limit for various materials (Neuber, 1968)

2.3 Modified Notch Rounding Approach

Seeger and co-workers modified the notch stress approach in an attempt to obtain better definitions of mean fatigue strengths and scatter ranges (Köttgen et al., 1991; Olivier et al., 1989 and 1994).Taking structural mild steel (St52-3 or S355) as an example, they fixed the notch rounding to *r* = 1 mm independently of the actual radius which varied around this value. The notch stress was determined for this value both at weld toes and roots without further corrections regarding the micro-structural support effect.

The resulting fatigue strength, expressed in terms of elastic notch stresses, was derived from fatigue tests and notch stress analyses of various T- and Y-joints, led to a simple design S-N curve, which could be applied to the structural component under consideration. Further details are given in Section 4.

2.4 Small Size Notch Approach for Plates with Thickness < 5 mm

The approaches described above assume a notch rounding with a reference radius of 1 mm, which may cause problems in thin structures, less than 5mm thick. In particular, the groove created by this radius at the weld toe or root causes a substantial reduction in cross-section and hence modifies the stress distribution, which affects the results of the fatigue assessment.

Therefore, a *small-size notch approach* which uses a reference radius r_{ref} = 0.05 mm has been proposed for assessing welded joints in thin-sheet material (steel or aluminium alloys). In a similar way to the r_{ref} = 1 mm approach, alternative design S-N curves based on notch stresses calculated assuming r_{ref} = 0.05 mm have been derived from fatigue test results from welded specimens, which are applicable to relevant well-defined groups of welded joints and materials, as shown in Section 4.

2.5 Approaches for Multiaxial Stress States

If the welded joint is subjected to more than one stress component, e. g. to axial and shear stresses acting in the plate adjacent to the weld, it is necessary to distinguish between:

1. loading that produces constant principal stress directions, which is usually associated with proportional stress components;

2. loading that produces principal stresses that change direction , i. e. non-proportional stress components, as produced, and indeed generally simulated in tests, by out-of-phase loading components

In the first case, the superimposed notch stress range can be computed directly and assessed in a similar way to the case of uni-axial loading. For simplification, in such cases the largest *principal stress range* in the most critical direction may be considered as the relevant fatigue parameter. In this case, the *equivalent stress range*, computed with the ranges of the notch stress components, is smaller. However, if the welded component is subjected to pre-dominantly in-plane shear load, the equivalent von-Mises stress can be larger than the maximum principal stress. For such cases, which are characterized by the second principal stress having a different sign, use of the equivalent von-Mises stress is recommended. Alternatively, the individual stress components may be assessed by interaction formulae, e. g. the Gough-Pollard ellipsis for combined normal and shear stresses (Sonsino and Wiebesiek, 2007). Reference is made to Hobbacher (2007) and to more recent literature in this field as it is still under development.

If the notch stresses are computed with stress concentration factors applied to the different stress components, account should be taken of the fact that the locations of the corresponding peak stresses might differ.

Table 2.1: Stress Types to be used in the Case of Multiaxiality

	First (max.) principal stress range	Equivalent von-Mises stress using ranges of stress components	Interaction formula with normal and shear stress ranges
Proportional loading	Yes, if second principal stress has same sign	Yes (with reduced S-N curve, see 4.1)	Yes (see Hobbacher, 2007; Sonsino & Wiebesiek, 2007)
Non-proportional loading with changing principal stress directions	No	No	Yes (see Hobbacher, 2007; Sonsino & Wiebesiek, 2007)

In the second case, the fatigue damage may be different due to the changing directions of the principal stresses with time. Therefore, at present it is generally recommended that the notch stress

ranges due to the individual stress components are assessed by an interaction formula, as indicated in Table 2.1.

3 Numerical Analysis of Notch Stresses

Usually, the notch stress is computed numerically using the finite element or the boundary element method. As an alternative, published parametric formulae are available for standard cases which have been derived mainly from numerical analyses. Both cases are considered in this Section.

3.1 Numerical Methods (FEM, BEM)

The objective of the numerical analysis is the computation of the stress concentration in the fatigue-critical notch under specified loads assuming linear-elastic material behaviour. This is a relatively simple task in view of the powerful methods available today, requiring mainly a sufficiently fine discretization of the structure in the notch area. A linear-elastic analysis is in most cases sufficient. However, effects of large displacements on the structural stress might be important, particularly in thin-walled structures, in which case geometrically non-linear structural stress analysis would be required. Contact problems may also require a non-linear analysis. However, contact between non-welded root faces is not usually assumed, leading to conservative results.

The finite element method (FEM) is the most likely choice for stress analysis today, where the structure is subdivided into a large number of small elements which are connected at nodes. The elements are characterized by definite shape functions for the displacements between the nodes and by the elastic material properties. An equation system is established and solved with respect to the nodal displacements (inclusive of rotations where applicable). These are later used to compute the stresses in the elements at the integration points depending on the shape function (e. g. linear or quadratic) and extrapolated to the nodal points. Details of the method and the different element types can be found in various textbooks, such as Hughes (1987), Bathe (1995), Zienkiewicz and Taylor (2000) or Cook et al. (2002).

The boundary element method (BEM) utilizes the possibility of mapping the elastic behaviour of a body on its surface so that only this has to be described and discretized by elements. It allows a much simpler input of geometrical data. The unknowns are either the tangential and normal displacements at the boundaries, which can be linear or quadratic within the elements, or, if these are prescribed, the tangential and normal external stresses. After solving the equation system, the displacements and internal stresses are determined at the boundaries as well as within the body. Details of the method are described among others by Brebbia et al. (1984), Cruse (1988), Banerjee (1994) and Gaul et al. (2003).

In view of its widespread application, most of the following descriptions will refer to the finite element method. The recommendations can accordingly also be transferred to the boundary element method by using models with corresponding element sizes and properties at the boundaries.

The stresses may be solved by a 3D or a 2D analysis, the latter being restricted to special cases, of the kind mentioned in Section 3.5, where variations of the geometry and loading in the 3rd direction can be neglected. In this case, plane strain conditions are usually assumed as biaxial stresses occur in the notches due to restraint in the 3rd direction.

3.2 Links to the Structural Stress Analysis

The stress concentration effect of a weld toe is limited to the vicinity of the local notch, so that it can be considered by a weld factor K_w superimposed on the undisturbed structural stress σ_{hs} at the hot spot. This allows the use of a structural hot-spot stress analysis with its corresponding model as the first step in the notch stress analysis. The latter can be performed with a refined local model using the sub-model technique where the stresses or displacements taken from the structural stress analysis are applied as boundary conditions. Alternatively, the super-element technique may be applied where the refined local model is inserted in the overall model. Also structural and/or notch stress concentration factors can be applied if they are available for the welded detail under consideration.

3.3 Modelling of the Weld for Notch Stress Analysis

When modelling the weld, two cases of application can be distinguished:

1. an idealized weld profile, characterized by a constant flank angle and the radius of the weld toe or root either by a reference radius (e. g. r_{ref} = 1 mm) or the actual notch radius

2. the actual weld profile, originating from measurement, which is idealized by a shape consisting of circular and straight parts

These two cases are dealt with in more detail in the following.

3.3.1 Modelling of idealized weld profiles

Fig. 3.1 shows the rounding of weld toes of butt- and fillet welds, characterized by the weld toe radius r and the weld flank angle θ. The rounding of the roots of non-penetrating fillet welds is shown in Fig. 3.2. The length of the non-welded root faces is retained by locating the vertex point of the circle at the weld root, see Figs. 3.2 and 3.3. Two shapes are usual, the keyhole notch and the U-shaped notch, see Fig. 3.2b and c. The latter reduces the high stress concentration in the keyhole notch for loading parallel to the non-welded root faces but it should be noted that it can also lead to an underestimation of the required notch stress for assessing potential fatigue failure in the weld throat (Fricke et al., 2008). An idealisation for a permanent backing bar of a butt joint with keyhole notches is shown in Fig. 3.4.

In thin-walled structures it might be necessary to compensate for the increase in net section stress due to the notch depth, see sub-section 3.5.2.

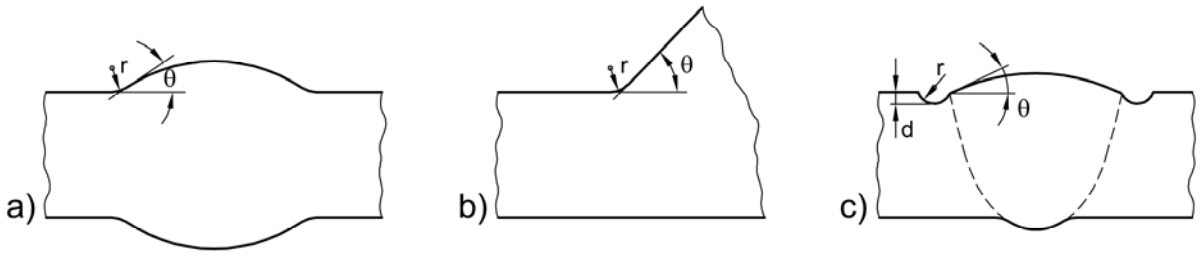

Fig. 3.1: Rounding of weld toes of a butt-weld, a fillet weld and a butt weld with undercuts of depth *d*

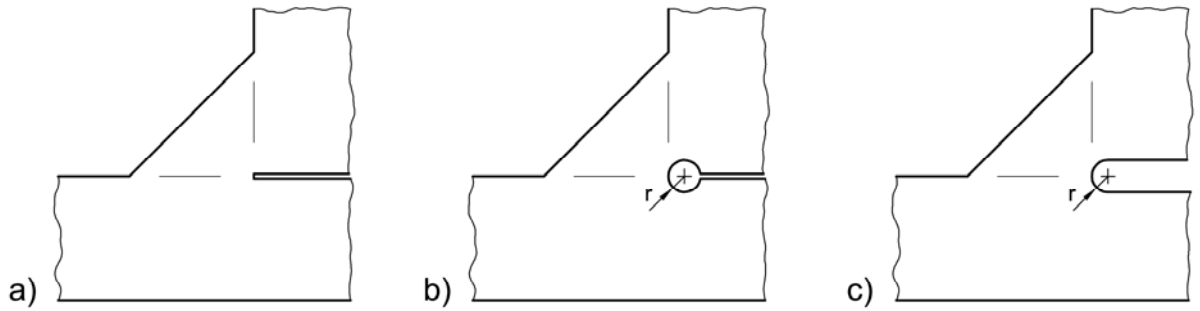

Fig. 3.2: Rounding of the weld root of a non-penetrating fillet weld by a keyhole and an U-shaped notch

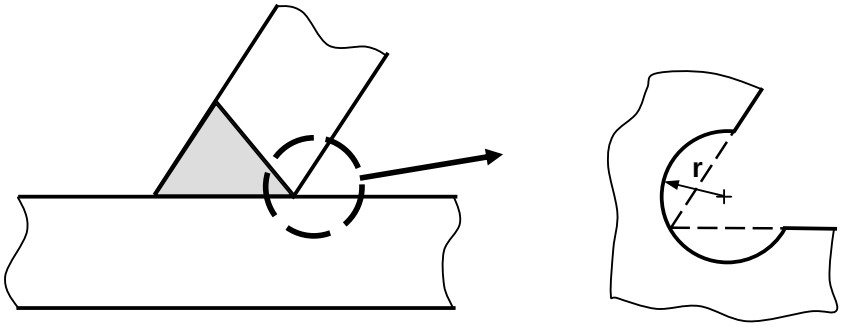

Fig. 3.3: Notch rounding of the weld root of a Y-joint

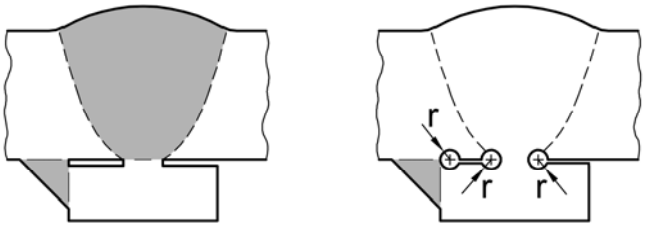

Fig. 3.4: Rounding of the weld root of a butt joint with permanent backing bar with keyhole notches

3.3.2 Modelling of the actual weld profile

A point-wise measured, actual weld profile is usually smoothened in a first step by arranging curved and straight parts of a surface with tangential transitions to avoid unrealistic stress peaks in concave corners. A radius followed by a straight line may be enforced at the weld toe to derive the primary geometric parameters, i. e. the weld toe radius r and angle θ, Fig. 3.5. Procedures for the derivation of these parameters have been developed (Lieurade et al., 2003).

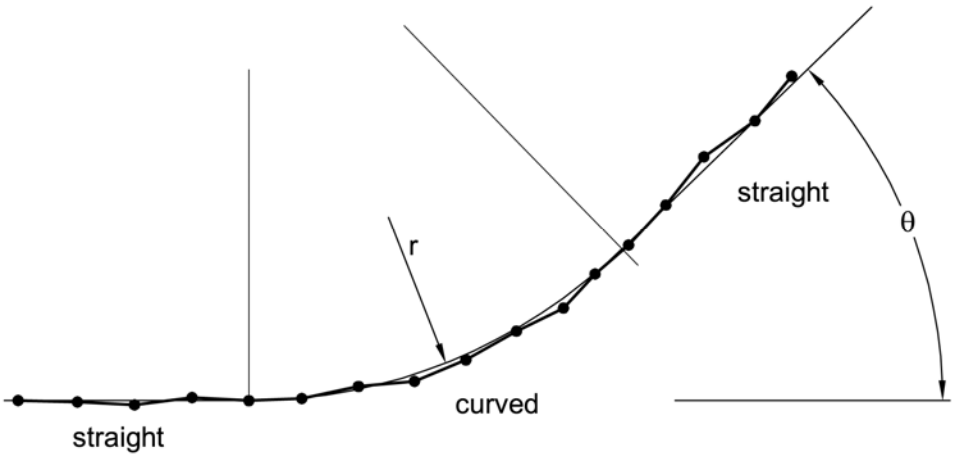

Fig. 3.5: Approximation of a measured weld profile by an idealized shape

Depending on the type of the approach chosen, the radius might have to be fictitiously enlarged to consider micro-support effects of the material.

3.4 Stress Analysis using Mesh Refinement

Usually, the discretization of the structure is performed such that a relatively coarse overall mesh is established, which is locally refined in the neighbourhood of the notches under consideration. The

overall meshing must take into account the force flow and deformation behaviour of the overall structure in order to obtain appropriate loading of the notched areas. In particular, the bending behaviour of structures has to be considered by appropriate elements and subdivision.

The mesh should be gradually refined towards the notched area, avoiding large steps in element size and excessive element distortion. The objective is to produce a mesh at the notch which is fine enough to model the steep stress increase normal and tangential to the notch surface and so yield the notch stress with sufficient accuracy. Figs. 3.6 and 3.7 show examples of meshes that achieve this objective.

For weld toes with an angle θ = 45° (Fig. 3.6), it is recommended that at least three elements with quadratic displacement function are arranged along the curve of the radius, which means a maximum element length of 0.25 mm in the case of a 1mm radius. The number of elements should be increased if they are of the linear displacement function type. Since the stress peak might be close to the transition between the radius and adjacent straight parts, it is advisable to continue with the same element length on the straight side before gradually increasing it.

Similarly, because there is also a steep stress gradient normal to the surface, the element length should be the same or smaller in this direction. By arranging approximately quadrilateral elements, the mesh will become gradually coarser as shown in Fig. 3.6.

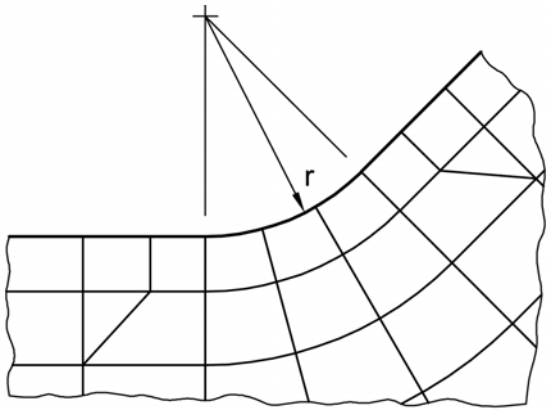

Fig. 3.6: Typical mesh for the notch stress analysis with elements having quadratic displacement function at a weld toe

In the case of a 3D model, the element subdivision in the third direction, i. e. along the weld length, should be chosen in accordance with the stress gradient expected. If the gradient is small, relatively long elements should be suitable.

The recommended element sizes for the two radii mentioned in the previous Section are summarized in Table 3.1. The numerical error is of the order of just a few percent if these limit values are used.

Corresponding recommendations are embodied in the mesh shown in Fig. 3.7, where the weld root region is modelled by a keyhole shape.

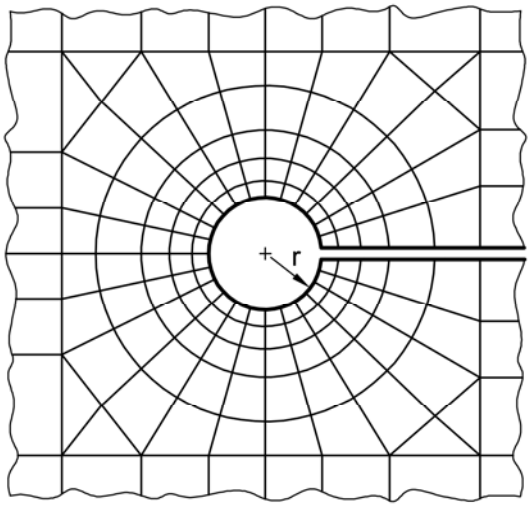

Fig. 3.7: Typical mesh for a notch stress analysis with elements having a quadratic shape function at a weld root modelled with a keyhole shape

Notch stresses are evaluated on the rounded surface of the notch, where a plane stress state exists, using the tangential and normal stresses in the section and the shear stresses on the notch surface. From these, principal or equivalent stresses can be derived.

Usually, nodal stresses are obtained from the computer program output. Special attention is drawn to the use of simple linear elements with constant stress distribution, where appropriate stress extrapolation to the free notch surface might be necessary. A check should be made that the stress distribution approaching the surface is smooth, otherwise the mesh might be too coarse.

Table 3.1: Recommendations for element sizes (along and normal to notch surface)

Element type (displacement function)	Relative size	size for r = 1 mm	size for r = 0.05 mm	No. of elements over 45 deg arc	No. of elements over 360 deg arc
quadratic (e.g. with mid-side nodes)	$\leq r/4$	$\leq$ 0.25 mm	$\leq$ 0.012 mm	$\geq$ 3	$\geq$ 24
Linear*	$\leq r/6$	$\leq$ 0.15 mm	$\leq$ 0.008 mm	$\geq$ 5	$\geq$ 40

*) The stress should be extrapolated to the free edge

3.5 Stress Analysis using Sub-models or Super-elements

In view of the extensive mesh generation effort required for mesh refinement, the analysis is frequently performed using the sub-model or alternatively the super-element technique.

In the *sub-model technique*, the analysis is performed in two steps:

1. Computation of deformations and stresses in an overall, coarse model suitable for the computation of structural stresses (example in Fig. 3.8a, being further described in 5.3)

2. Computation of notch stresses in a fine-meshed sub-model, which is loaded by prescribed displacements or stresses at the boundaries taken from the overall model; in the example in Fig. 3.8, the uppermost flat part is considered because it is the most highly stressed under bending of the hollow section about its horizontal axis.

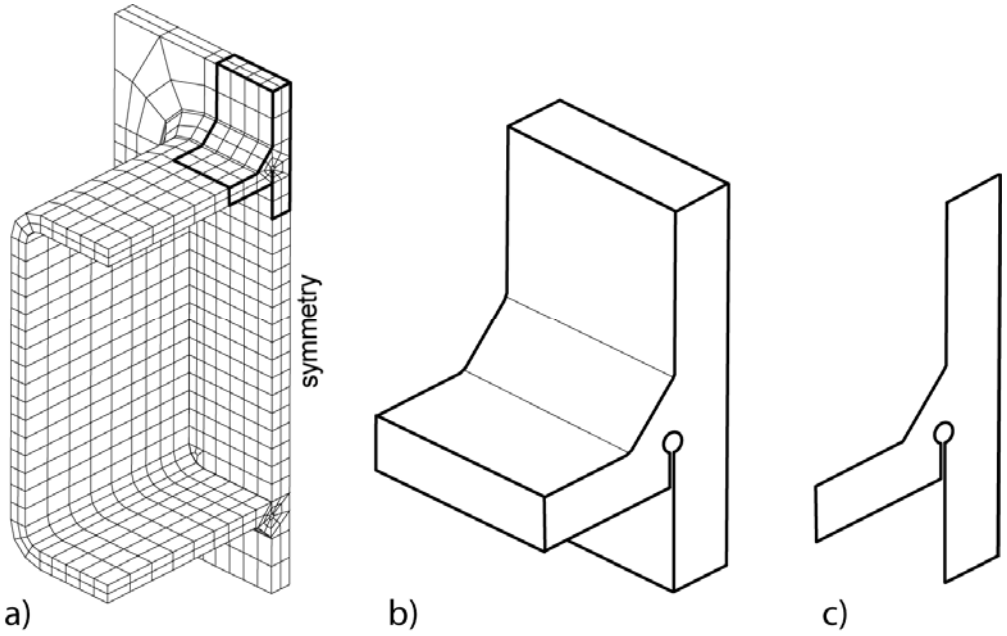

Fig. 3.8: a) Overall finite element model of a fillet-welded end joint of a rectangular hollow section and b) extent of a volumetric sub-model and c) 2D-sub-model

The sub-model may be a volumetric model (Fig. 3.8b) or, if the stresses are acting mainly in the plane normal to the weld line, a 2D-model assuming plane strain conditions (Fig. 3.8c). The requirements on element sizes etc. are the same as those given in the preceding sub-section. The extension of the sub-model should be chosen such that boundary effects on the notch stresses are negligible.

The loading of the sub-model consists in most cases of the application of the nodal displacements originating from the overall model. Local loads such as pressure also need to be considered. As the overall model consists of a coarser mesh, the displacements must be interpolated between the nodal points in an appropriate way. The sub-model technique that includes the interpolation to achieve compatible displacements at the boundary of the sub-model is supported by some finite element programs.

The alternative to the prescription of boundary displacements is the application of sectional forces and moments or stresses at the boundaries, again taken from the overall model. This method, which has frequently been applied to 2D sub-models, has the advantage that the loading of the connected structural components is clearly evident. The loading has to be in equilibrium as far as possible. Non-equilibrated forces or moments can occur due to shear forces acting in the cross section. These have to be taken by supports which should be arranged in an area where their effect on the notches is minimal.

A very important requirement for obtaining the same results as with mesh refinement is that the overall model should have the same stiffness in the relevant part as the sub-model. Otherwise, the notch stresses will be wrong. For example, if the overall model has a higher stiffness in the area under investigation than the sub-model, which is frequently the case, the notch stresses

- will be too small if prescribed displacements are arranged at the boundaries, because the latter are under-estimated by the stiffer overall model

- might be too large if forces and moments (or internal stresses) are applied at the boundaries, because these can be overestimated by the overall model (particularly in the case of statically indeterminate structures).

The relevant part of the overall model should be created in such a way that local deformations can fully develop, in particular local bending which might be partly prevented by the element behaviour. In the case of non-penetrating welds, the non-fused region should be included in the overall model and the weld should be able to deform in the same way that it does in the sub-model. Fig. 3.8 gives an example of such a global model, showing the refined mesh of the fillet weld.

Appropriate modelling can be checked by comparing the stresses at the boundaries of the sub-model with those in the overall model, which have to be the same if the displacements at the boundaries are prescribed. If the forces and moments (or internal stresses) are prescribed, the boundary displacements must be the same.

The *super-element technique* (and the historically earlier *substructure technique*) differs from the sub-model technique insofar as the local model is inserted into the overall model as a 'super-element'. This avoids the problems mentioned with respect to different stiffnesses of the sub-model and the respective part of the overall model. Here it is also important that the extent of the super-element is chosen in such a way that boundary effects on the notch stresses are negligible. Furthermore, compatible displacement functions have to be ensured at the connection between the super-element and the surrounding structure, which is possible with special coupling elements in some programs. It is recommended to check the accuracy of the results.

3.6 Special Aspects

3.6.1 2D vs. 3D Analysis

In several cases, a 2D analysis is sufficient, which greatly simplifies the modelling. The following pre-requisites should be fulfilled for a 2D analysis:

- The loading of the weld should act mainly in the plane perpendicular to the weld line, which means that normal and shear stresses along the weld can be neglected
- The geometry of the weld should not change in the area considered so that a representative geometry can be chosen

As mentioned before, plane strain conditions should be imposed on the 2D model as the contraction in high stress concentration notches is restrained normal to the plane modelled. As a consequence, a biaxial stress state occurs at the notch surface.

Methods for determining the notch stress concentration at welds in cases of multiaxial loading, inclined welds and weld ends based on 2D models (mainly cross-sectional) are described by Radaj et al. (2006), pp. 135-142 and 150-152. These methods may be appropriate where a 2D notch stress analysis by FEM or BEM is too expensive or time-consuming.

3.6.2 Compensation for fictitious radius in thin-walled structures

As noted earlier, the introduction of the fictitious 1mm radius can increase the net section stress in thin material and thus lead to an over-estimate of the notch stress. The problem is particularly acute at the weld root. To compensate, Radaj et al. (2006) give the following reduction factors to be applied to the fatigue notch factor K_f (and hence, to the notch stress) for cases based on internal forces and moments, where it is necessary to distinguish between a one-sided notch (eq. 3.1 and Fig. 3.9a,b) and a two-sided notch (eq. 3.2 and Fig. 3.9c,d):

$$K_f^* = \frac{(1-\rho_f/t)^2}{1+(1+\sigma_l/\sigma_u)\,\rho_f/t}\,K_f \qquad (3.1)$$

$$K_f^* = \frac{2\,(1-\rho_f/t)^2}{1+(1+\sigma_l/\sigma_u)\,\rho_f/t}\,K_f \tag{3.2}$$

where K_f^* is the reduced fatigue notch factor and the other terms are described in Fig. 3.9. It should be noted that the correction might be too large e. g. in cases with additional restraint of the surrounding structure. In such cases an additional computation with a shifted notch, keeping the net section, is recommended to derive the correction factor.

Additional modifications have been proposed to consider the effect of gap closure in overlap joints and for the interaction of fictitious notch radii that are too close together.

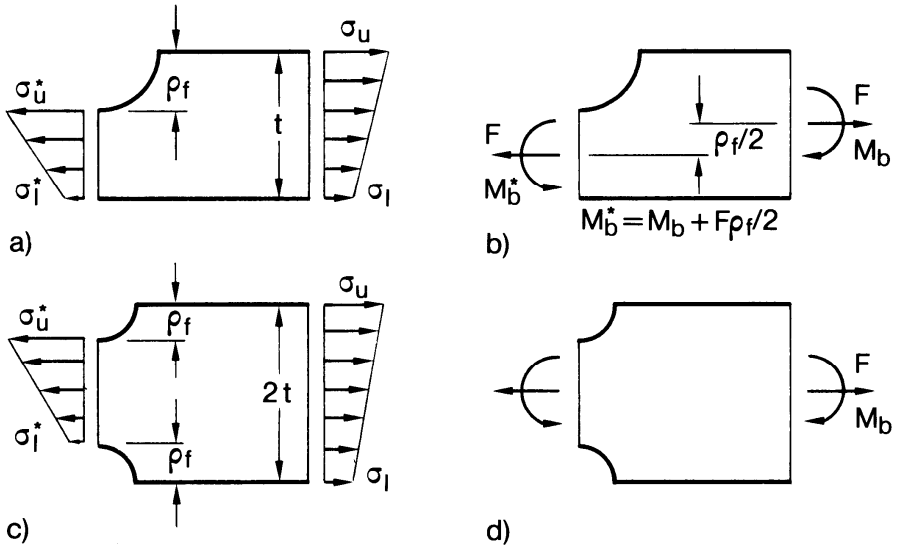

Fig. 3.9: Modification of the membrane and bending stress by fictitious notch rounding with undercut at one side (a,b) or at both sides (c,d), after Radaj et al. (2006)

3.6.3 Consideration of misalignment and other imperfections

In numerical stress analyses, perfectly-aligned structures are usually assumed, However, axial and angular misalignments may substantially increase the local stresses and have, therefore, to be considered in the notch stress analysis (as also in the structural hot-spot stress analysis), see Hobbacher (2007).

Generally, two alternatives exist for the consideration of misalignment effects:

1. Inclusion of the misalignments in the model, based for example on specified fabrication tolerances, measured values or worst-case assumptions

2. The application of stress magnification factors, which are usually related to the applied axial stress components. Typical stress magnification factors for those joints which are particularly affected by misalignment are given by Hobbacher (2007)

If the numerical analysis is performed in two steps, i. e. the computation of the structural stresses or overall deformations in the first step, from which the notch stresses are derived in the second step, the magnification factors are only applied once.

Concerning other imperfections, it should be noted that the fatigue classes presented in Section 4 were derived on the basis of idealized numerical models of welds with relatively good quality toe profiles, with no significant undercut or other features that introduce sharp section changes. More severe imperfections such as deeper undercut or cold laps need to be modelled accordingly, e. g.

as shown in Fig. 3.1c (Gosch and Petershagen, 1997). Both types of imperfections can also be analysed using the crack propagation approach.

3.7 Parametric Formulae for Notch Stress Concentration Factors

Parametric formulae have been published for several standard cases, such as butt joints, T-joints and both load-carrying and non-load-carrying cruciform joints. Examples include Anthes et al. (1993), Brennan et al. (2000), Iida and Uemura (1995), Lawrence et al. (1981), Lehrke (1999), Radaj and Zhang (1991), Rainer (1983) and Tsuji (1990). An application is shown in Section 5.1.4.

4. Fatigue Strength

4.1 Design S-N Curves for Reference Radius of 1 mm

The notch stress approach was first linked only to the endurance limit, defined as the fatigue strength at $2 \cdot 10^6$ cycles. In this respect, for consideration of welded joints, Radaj (1990) proposed application of the fatigue strength of low strength steels in the non-machined condition, which corresponds to a stress range of 240 MPa at $2 \cdot 10^6$ cycles for a stress ratio $R = 0$ and a survival probability $P_s = 90\%$.

The extensive programme of fatigue tests on welded joints performed in connection with Seeger's approach (Olivier et al., 1989 and 1994), see Section 2.2, provided further information about the scatter in fatigue lives and the effect of the stress ratio R. Fig. 4.1 shows good correspondence to a Gaussian distribution.

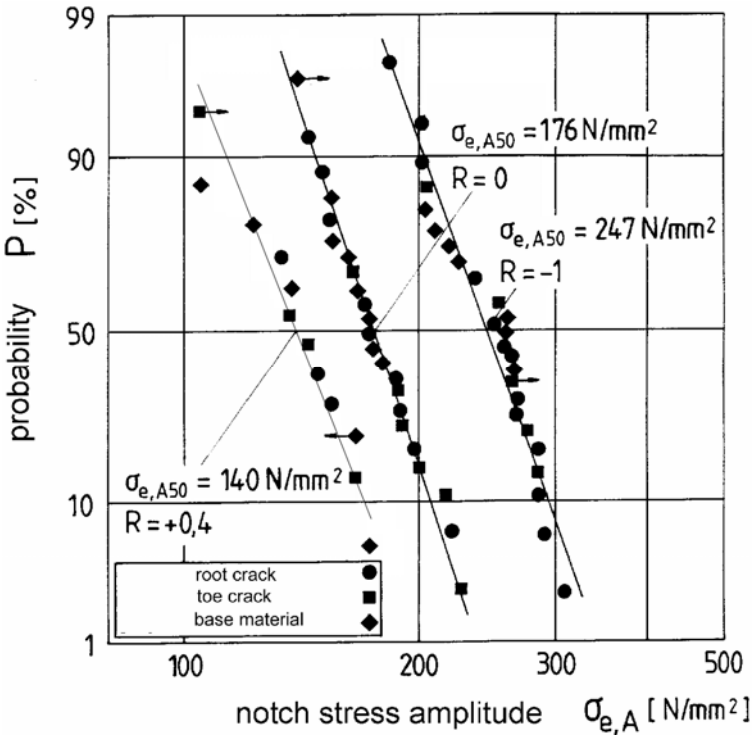

Fig. 4.1: Notch stress fatigue strength at $2 \cdot 10^6$ cycles for stress-relieved T- and Y-joints from test results by Olivier et al. (1989 and 1994)

The original endurance limit approach was subsequently converted to one based on S-N curves on the basis that such curves should be of the form $\Delta\sigma^m \cdot N = C$, where $\Delta\sigma$ is the notch stress range and the constant $C = (\mathrm{FAT})^m \cdot 2 \cdot 10^6$, FAT being the fatigue strength at $2 \cdot 10^6$ cycles. As generally assumed for welded joints, the slope exponent of $m = 3$ was selected. This allows the IIW fatigue classes defined for the nominal, structural hot-spot and effective notch stress approaches to be compatible with each other, as their S-N curves all have the same slope.

The FAT value to be used for the effective notch stress approach S-N curve was derived from a statistical analysis of relevant fatigue test results obtained from welded joints. In order to allow for the presence of high tensile residual stresses in actual welded components and structures, particular attention was paid to fatigue data obtained under high stress ratios, such as those at $R = 0.4$ in Fig. 4.1. Further evaluation of these and other results (Hobbacher, 2008, see Fig. 4.2) shows a characteristic fatigue strength (stress range) of FAT 225 for a survival probability $P_s = 97.7\%$. For aluminium alloys, a corresponding value of FAT 71 (Morgenstern et al., 2004) and for magnesium

a value of FAT 28 may be assumed (Karakas et al., 2007). The values are summarized in Table 4.1. It should be noted that these fatigue classes and the assumption that the S-N curve has a slope of m = 3 are only valid for sharp notches with a fictitious rounding of 1 mm, as proposed in Seeger's approach and as 'worst case' in Radaj's approach.

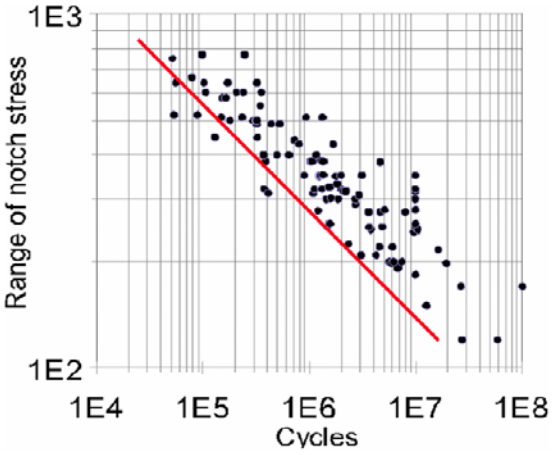

Fig. 4.2: Re-analysis by Hobbacher (2008) of test data by Olivier et al. (1989) and Köttgen et al. (1991) for T- and Y-joints subject to different loading modes with R ≥ 0.4, root and toe failure

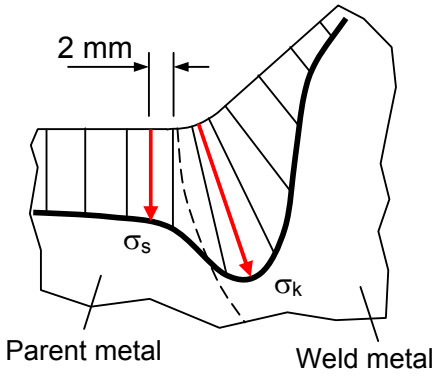

Fig. 4.3: Stress distribution at a weld toe

.

Table 4.1: Characteristic fatigue strength for welds of different materials based on effective notch stress with r_{ref} = 1 mm (maximum principal stress)

Material	Characteristic fatigue strength (P_s = 97.7%, $N = 2 \cdot 10^6$)	Reference
Steel	FAT 225	Olivier et al. (1989 and 1994) and Hobbacher (2008)
Aluminium alloys	FAT 71	Morgenstern et al. (2004)
Magnesium	FAT 28	Karakas et al. (2007)

The scatter in the fatigue data that led to the recommendations in Table 4.1 amounted to a scatter ratio of 1.5 between the fatigue strengths for survival probabilities of 90% and 10%, which corresponds to a standard deviation of $\log\Delta\sigma$ of 0.0687 and with the slope exponent of the design S-N curve of m = 3 to a standard deviation of $\log N$ of 0.206. This allows alternative S-N curves based on other survival probabilities to be derived.

It is emphasized that the FAT classes are based on the maximum principal stress in the notch. If the von Mises equivalent stress is used, a correspondingly smaller FAT class applies, because the equivalent stress is usually smaller in sharp notches. This subject is currently under investigation but meanwhile a reduction by at least one fatigue class is recommended.

It should be noted that the so-called thickness correction, which is applied in the nominal and structural hot-spot stress approaches to welded plates more than 25mm thick, is already included in the effective notch stress. This is because the notch stress is governed by the ratio r/t, such that it increases with increased thickness t. Regarding consideration of misalignment and weld imperfections, note the remarks in 3.6.3.

4.2 Correction for Mild Weld Notches with Reference Radius of 1 mm

A problem arises for relatively mild notches which, despite the radius of 1 mm, have a low notch stress concentration factor. Such cases have not been verified by the aforementioned fatigue tests. The problem can easily be understood by considering transverse butt welds with almost no weld overfill. The corresponding weld toe notch stress concentration factor will be close to unity but the fatigue class is certainly far below FAT 225. Mild notches may generally occur at weld toes that have been ground, have small flank angles and/or are in thin plates.

The notch factor K_w of a weld is defined as the ratio of the effective notch stress σ_k to the structural stress σ_s, see also Fig. 4.3:

$$K_w = \sigma_k / \sigma_s \tag{4.1}$$

where the structural stress can be determined either with the methods proposed elsewhere (e. g. Niemi et al., 2006) or from the notch stress distribution, taking the stress value at a distance of 2 mm from the transition between straight and curved part (without further thickness correction).

It is proposed as a preliminary approach to assume a notch factor K_w of at least 1.6 in connection with the aforementioned fatigue classes. This means that both the structural hot-spot stress and the effective notch stress at a weld toe need to be checked and the latter assumed to be 1.6 times the former if it is found to be less.

As with the nominal and structural hot-spot stress approaches, the fatigue strength of a welded joint is limited by the parent material S-N curve in the lower endurance regime (e.g. FAT 160 S-N curve with a slope exponent m = 5 for steel). To allow for this in the effective notch stress approach, the fatigue strength of the parent material must additionally be checked using the structural stress σ_s at the weld toe and the corresponding material S-N curve.

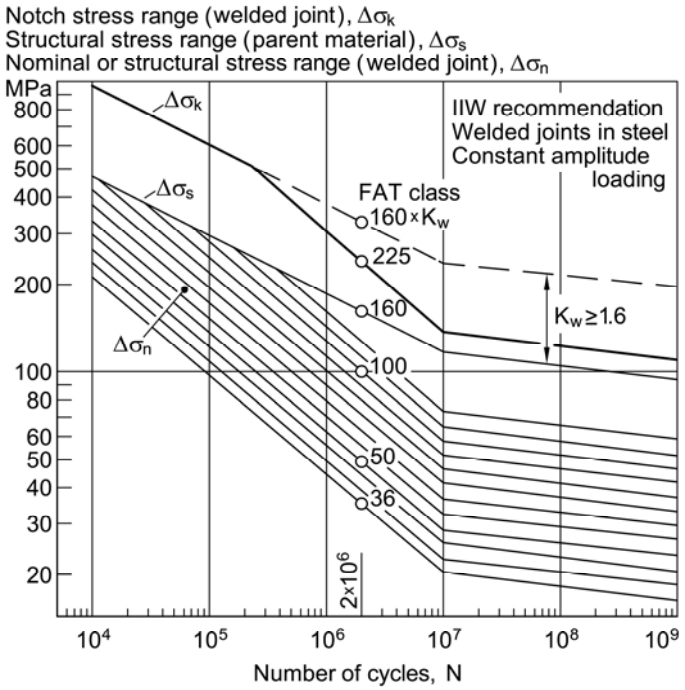

Fig. 4.4: S-N curves of fatigue classes in terms of nominal, structural (FAT 160) and notch stress (FAT 225) compared with FAT class 160 x weld shape factor K_w (Radaj et al. 2008)

Fig. 4.4 compares the various IIW S-N curves for steel to illustrate how the S-N curve governing the fatigue strength varies with endurance. The parent material FAT160 curve multiplied by the notch factor K_w intersects the effective notch stress FAT 225 curve in this example at approximately 200,000 cycles, which means that the parent material governs design for smaller numbers of cycles. Obviously, this situation is particularly relevant in cases where K_w is small.

Finally it should be noted that the slope of the S-N curve is generally shallower for mild notches. This effect is at least partly considered by the aforementioned approach. Nevertheless, an approach with slope exponents changing with notch severity might be developed in future to better consideration of the local influencing factors.

4.3 Design S-N Curves for Mild Weld Notches with Larger Radii

Larger notch radii may be relevant for some welding processes or for welds subject to post-weld improvement treatment.

The S-N curves and fatigue classes mentioned in Section 4.1 are only valid for the reference notch radius of 1 mm. In view of the larger reference radius that results from the addition of 1mm to the actual radius (eq. 2.1), the notch stress needs to be assessed against a slightly reduced fatigue class. The characteristic fatigue strength proposed by Radaj for non-machined steel, i. e. $\Delta\sigma_k$ = 240 MPa for P_s = 90%, yields a value of 215 MPa for P_s = 97.7% if the usual standard deviation is assumed. A suitable fatigue class in the present IIW scheme would be FAT 200. A similar value was found in an evaluation of fatigue tests with brackets using the actual notch radius enlarged by 1 mm (Fricke and Kahl, 2007). It should be noted that such a fatigue class is still only valid for relatively sharp weld toe radii, e. g. 1 - 3 mm. This means that the procedure outlined in Section 4.2 and the assumption of a minimum notch factor K_w = 1.6 is still recommended for use in conjunction with the lower FAT200 S-N curve.

The approach described in Sections 4.1 and 4.2 has not been verified for larger weld toe radii as might arise in, for example, joints improved by grinding, peening or TIG-dressing. The logical approach is to assess the notch stress computed for such cases using the S-N curve for the weld or parent metal, whatever is relevant. However, since this may be affected by the post-weld treatment, a general recommendation is difficult and relevant published literature should be consulted. In addition, as described in Section 4.2, the parent material in front of the weld toe must be checked using the structural hot-spot stress and the parent material S-N curve.

Alternatively, the nominal or structural hot-spot stress approach with corresponding FAT classes may be applied to the welded joint (Hobbacher, 2007).

4.4 Design S-N Curves for the Small Size Notch Approach with Reference Radius of 0.05 mm for Plates < 5 mm Thick

The small-size notch approach was originally developed for spot welds in thin sheets and later extended to thin-sheet lap joints. Corresponding design S-N curves have been derived from fatigue test results obtained from welded specimens by Eibl et al. (2003) and Karakas et al. (2007), yielding the FAT classes given in Table 4.2. Again it should be born in mind that the notch stresses are theoretical values without consideration of local yielding of the material.

As before, the fatigue classes are based on the maximum principal stress in the notch of a 3D structure. Equivalent stresses should be assessed using a lower fatigue class.

Table 4.2: Characteristic fatigue strength for welds of different materials based on theoretical notch stress with r_{ref} = 0.05 mm (maximum principal stress)

Material	Characteristic fatigue strength (P_s = 97.7%, $N = 2 \cdot 10^6$)	Reference
Steel	FAT 630	Eibl et al. (2003), Sonsino (2008)
Aluminium alloys	FAT 180	Eibl et al. (2003), Karakas et al. (2007) , Sonsino (2008)
Magnesium	FAT 71	Karakas et al. (2007) , Sonsino (2008)

5. Demonstration Examples

The following presents the results of a round-robin study (Fricke, 2006) performed by members of IIW Working Group XIII-3 '*Stress Analysis*'. The objective was to identify sources of errors and scatter in results by performing the stress analysis for well-defined cases using different modelling techniques, analysis methods and computer programs. The following three structural details were considered:

1. A cruciform joint with fillet welds similar to the left part of Fig. 2.1 (2D case)
2. A T-joint between two rectangular hollow section members (3D case)
3. A fillet welded end connection of a rectangular hollow section member with non-fused weld root faces as shown in Fig. 3.7 (3D case)

A fourth example from the automotive industry illustrates the application of the small size notch approach. Further demonstration examples for notch stress analyses on welded joints are given by Radaj et al. (2006). Here, several design-related notch stress evaluations show the differences between the notch stresses in different weld types applied to the same type of welded joint.

5.1 Fillet Welded Cruciform Joint

5.1.1 Description of the detail

Fig. 5.1 shows the geometry and loading of the cruciform joint made from 12 mm thick plates. The fillet welds have a flank angle of 45 degrees and a throat thickness of 5 mm. The non-fused root faces, indicated by horizontal lines in Fig. 5.1, are assumed to have a length equal to the plate thickness (12 mm). Two alternative load cases (LC) are considered:

LC 1: Unit nominal stress σ_1 in the continuous plate, i.e. the fillet welds are non load-carrying and the most likely sites for fatigue cracking are the weld toes on that plate

LC 2: Unit nominal stress σ_2 in the attached plates, i.e. the fillet welds are load-carrying, in which case the potential sites for fatigue cracking are the weld toes in these plates or the weld roots.

Notch stresses are therefore required at the weld toes and at the weld root for a reference notch radius of r_{ref} = 1 mm in each case.

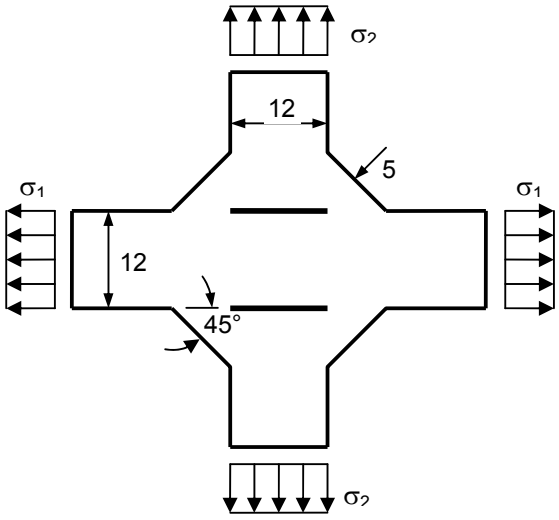

Fig. 5.1: Fillet welded cruciform joint

5.1.2 Description of the models and analysis results

In total seven analyses were performed, using the 2D finite element (FEM) and boundary element (BEM) methods, see Table 5.1. In all cases, the double-symmetry was utilised by analysing only a quarter of the structure. In five analyses, the weld root was rounded with a keyhole shape similar to Fig. 2.1 (also shown in the left part of Fig. 5.3), retaining the actual length of the gap. In the two remaining analyses, a U-shape with a gap width of 2 mm was used (see also the right part of Fig. 5.3).

Fig. 5.2 shows some typical meshes. The notches rounded with a radius of 1 mm were modelled using a large number of elements for increased accuracy. Figs. 5.3 and 5.4 give examples of typical stress results. The values given were obtained for a unit stress, i.e. they can be interpreted as stress concentration factors (SCFs) or fatigue notch factors K_f. It is interesting to note that the differences at the weld root between the keyhole and U-shape notches are rather large for LC 1, where the stress acts parallel to the gap and the weld is nominally non-load-carrying. The keyhole notch may overestimate the real notch effect as the upper and lower parts of the notch do not exist in the real structure. Compared e.g. with the crack propagation approach, where the stress intensity factor is rather small in this case, the U-shape seems to be the more realistic. On the other hand, this possible weld root stress overestimation is not relevant in the detail investigated, as the stress at the weld toe is more critical.

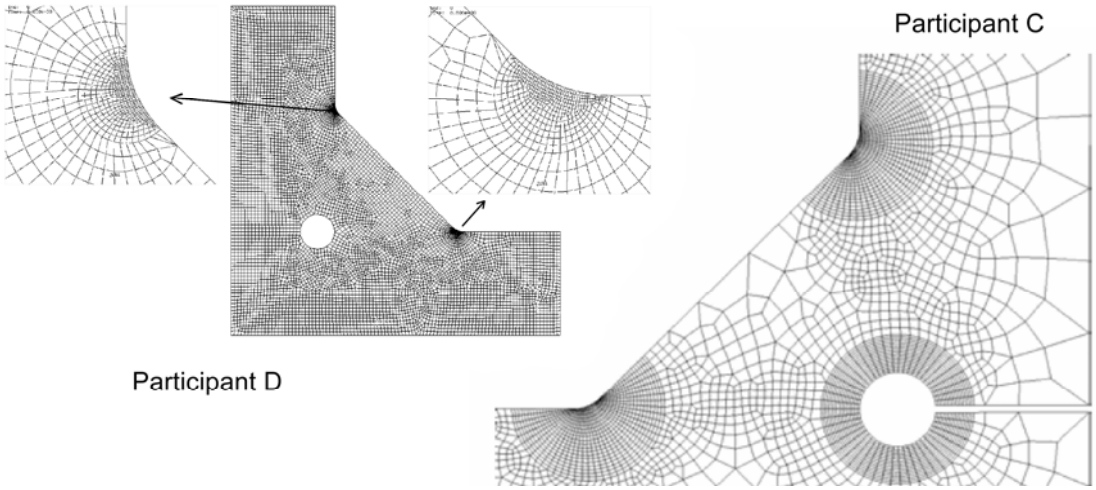

Fig. 5.2: Examples of FE meshes with keyhole shape (quarter models)

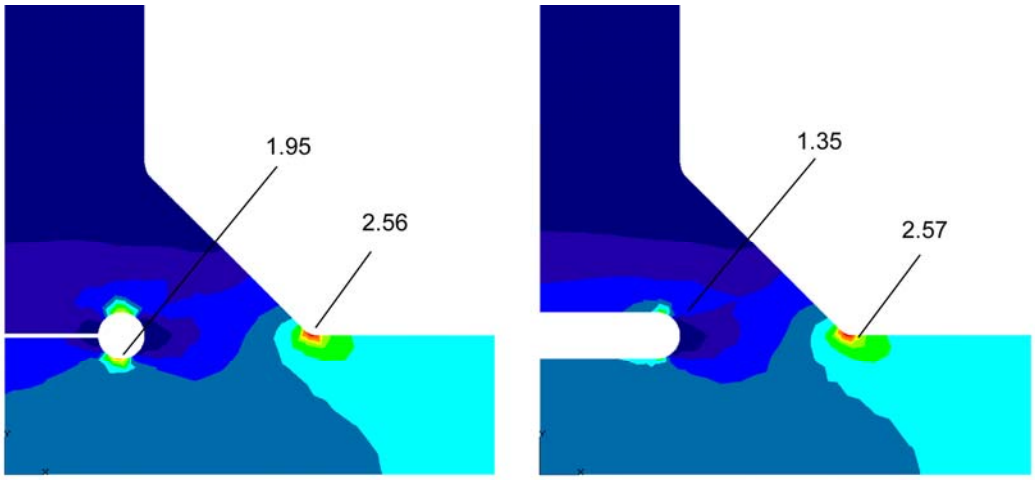

Fig. 5.3: Maximum principal stress distribution and notch stresses for LC 1 (Participant A)

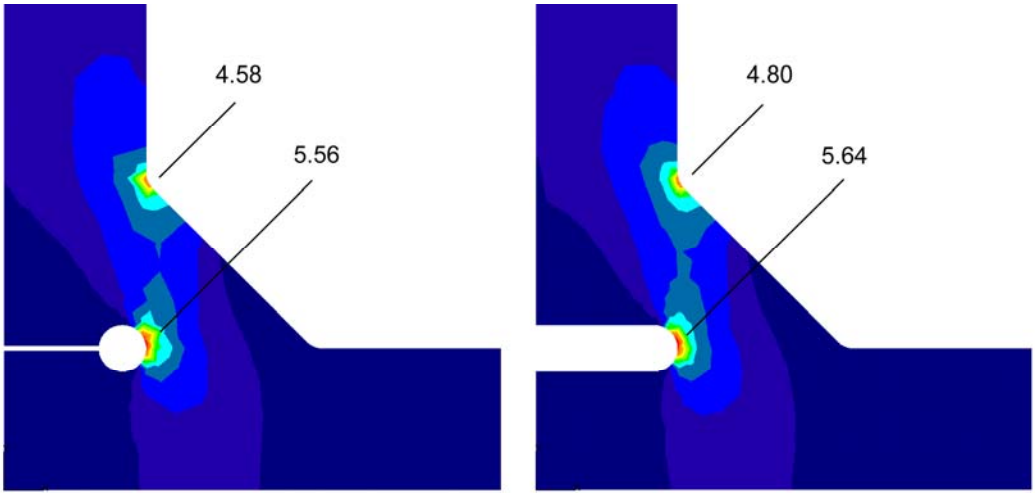

Fig. 5.4: First principal stress distribution and notch stresses for LC 2 (Participant A)

Table 5.1: Analysis results for the cruciform joint with fillet welds

Partici-pant	Weld root	Method / Program	Element type	Element length at toe / root	SCFs for LC 1		SCFs for LC 2	
					Toe	Root	Toe	Root
A	Keyhole	BEM / BEASY	quadratic	0.05mm / ~ 0.16mm	2.56	1.95	4.58	5.56
B	Keyhole	FEM / MSC Nastran	linear	0.04mm / 0.08mm	2.58	1.89	4.62	5.65
C	Keyhole	FEM / IDEAS	quadratic	~ 0.08mm / 0.12mm	2.53	1.95	4.52	5.56
D	Keyhole	FEM / MSC MARC	linear	0.017mm / ~ 0.16mm	2.42	1.99	4.05	5.40
E	Keyhole	FEM / ANSYS	quadratic	0.05mm / 0.05mm	2.56	1.96	4.57	5.71
Coefficient of variation for meshes with keyhole root					2.5%	1.9%	5.3%	2.1%
A	U	BEM / BEASY	quadratic	0.05mm / ~ 0.16mm	2.57	1.35	4.80	5.64
E	U	FEM / ANSYS	quadratic	0.05mm / 0.05mm	2.56	1.47	4.80	5.72
Coefficient of variation for meshes with U-shaped root					0.3%	6.0%	0%	1.0%

For LC 2, the differences between the keyhole and U-notch are very small. It is interesting to note that the notch stress at the weld toe is slightly affected by the modelling of the weld root. The U-notch is connected to a weaker structure, causing increased stresses at the weld toe.

5.1.3 Discussion of the results

The results in Table 5.1 are fairly close together, yielding very small coefficients of variation. This is due to the simple model and rather fine meshes. As mentioned before, fine meshes are required not only along the notch surface, but also normal to it, in order to model the steep stress gradient in the thickness direction, which was realised by all participants (see Fig. 5.2).

The stress deviates by more than 10% from the others in only one case, Participant D's toe stress for LC 2 (SCF = 4.05). The reason for this is not clear.

5.1.4 Comparison with parametric formulae

Parametric formulae given in the literature for the SCFs in cruciform joints may also be applied. These can be applied directly to LC 2. However, it is possible to consider LC 1 as a cruciform joint with full penetration welds and only calculate the stress at the weld toe. This is justified by the fact that the non-fused root faces have only a small effect on the notch stress at the weld toe.

The results for three approximation formulae are compared in Table 5.2 with each other and with the mean value of all computed SCFs from Table 5.1. The deviations are particularly large for the results based on Lawrence's formulae.

Table 5.2: Comparison between results from approximation formulae and computation

Method	SCFs for LC 1	SCFs for LC 2	
	Toe	Toe	Root
Formulae of Lawrence (1981)	2.21*	3.24	4.69
Formulae by Radaj and Zhang (1983)	n.a.	4.15	5.45
Formulae by Anthes et al. (1993),	2.77*	4.91	5.83
Mean value of computation (Table 5.1)	2.54	4.56	5.61

*) Computation for cruciform joint with full penetration welds

5.2 T-Joint between Two RHS Members with Weld Toe Failure

5.2.1 Description of the detail

The second detail comes from a competition organised by the American Society of Automotive Engineers (weld challenge 1, ref. SAE, 2003) concerning the prediction of the fatigue life of welded joints. The example, shown in Fig. 5.5, was a T-joint between rectangular hollow section (RHS) members in 345 MPa yield steel. The main continuous member had a quadratic section with outer dimensions of 4 x 4 inch (101.6 x 101.6 mm) while the connected member had a rectangular section of 2 x 6 inch (50.8 x 152.4 mm). Both tubes were 0.312 inch (7.9 mm) thick and had corner radii at mid-wall thickness of 0.486 inch (12.3 mm, or 16.3 mm at the outer surface. The weld leg length was 5/16 inch (7.9 mm). No information was provided about the weld penetration.

A number of joints were fatigue tested under alternating loading (R = -1). The right end of the continuous RHS member and the end of the connected member were fixed as indicated in Fig. 5.6. A horizontal force of 4,000 pounds (17.8 kN) was applied at the left end with a lever of 12.5 inch (317.5 mm) related to the centre of the RHS, creating horizontal shear, bending and torsion in the continuous member. The fatigue crack initiation point was at the upper weld toe in the connected tube, as indicated by the arrow in Fig. 5.7. The mean fatigue life observed in the experiments was about 75,000 cycles.

Numerical analysis and fatigue life assessment of the detail as part of the challenge were described by Kyuba and Dong (2003).

5.2.2 Description of the models and analyses results

Due to the need for a 3D model of the joint, only two participants analysed this detail. As notch rounding with 1 mm radius requires a very fine mesh, the finite element analysis was performed in two steps, as described in Section 3.5:

1. Coarse mesh analysis with shell or solid elements resulting in structural hot-spot stresses and deformations

2. Fine mesh analysis of the critical part using mesh refinement or the sub-model technique, where the sub-model is loaded by the deformations at the boundaries taken from the coarse model

Both participants performed the coarse mesh analysis using solid elements. Since precise details of the weld were not known, it was modelled as both a full penetration and a fillet weld. Figs. 5.8 - 5.9 and Table 5.3 show details of the models.

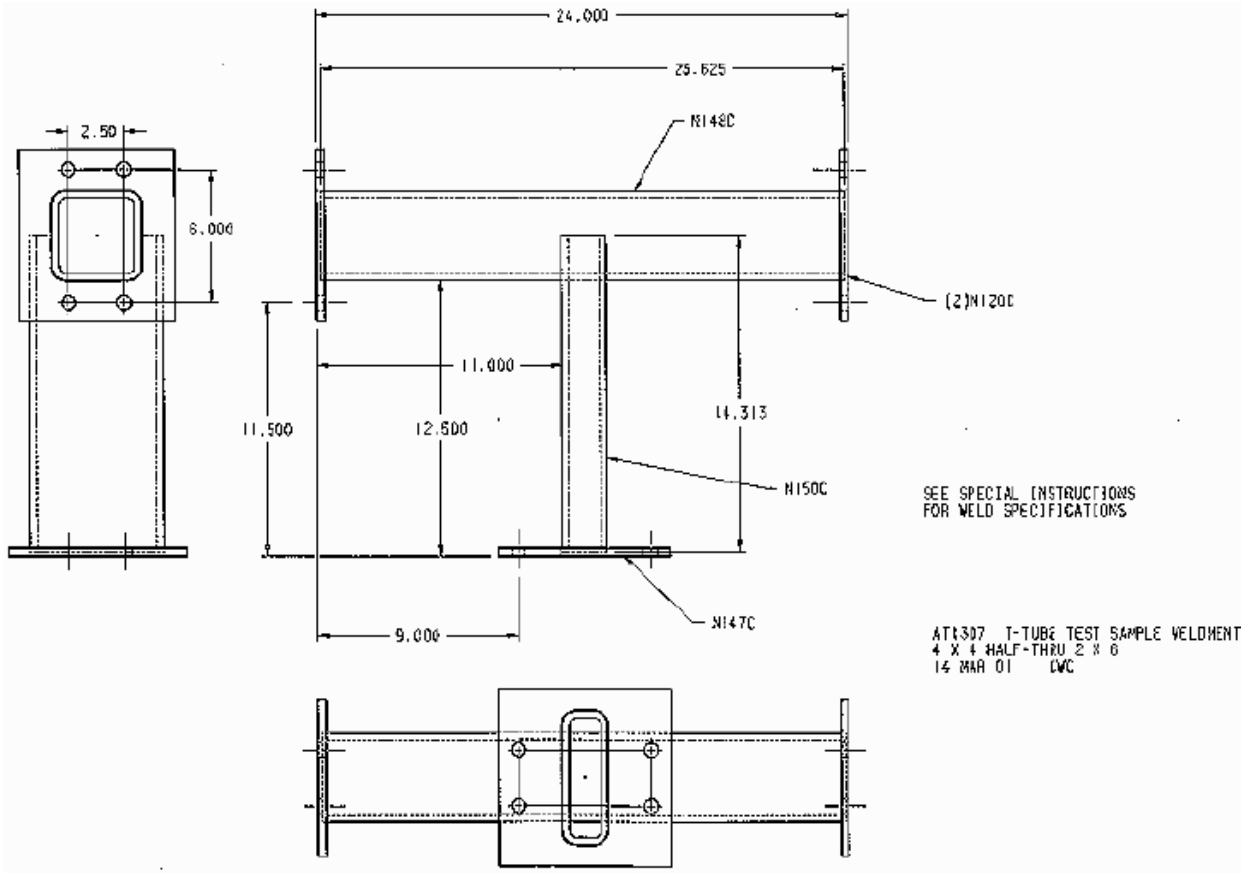

Fig. 5.5: Sketch of the RHS joint (SAE, 2003; units: inch)

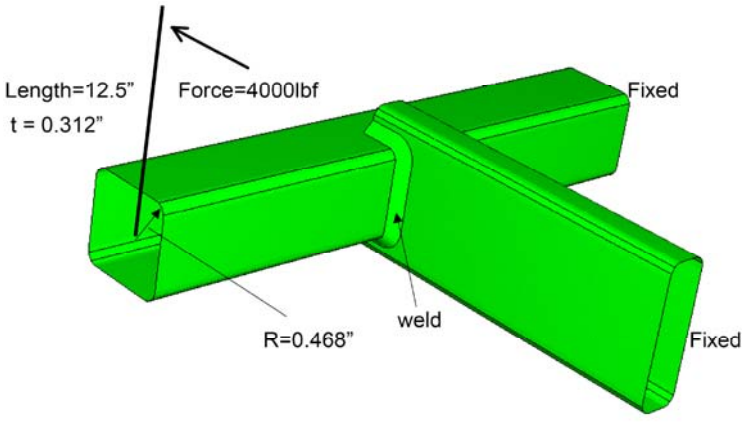

Fig. 5.6: Boundary conditions and loading of the joint

Fig 5.7: Crack location (SAE, 2003)

Table 5.3: Analysis results for the complex RHS joint (principal stress ranges)

Par-tici-pant	Program	Element type	Element length (at notch)	Full penetration weld		Fillet weld (zero penetration)	
				Struct. stress range [MPa]	Notch stress range [MPa]	Struct. stress range [MPa]	Notch stress range [MPa]
A	ANSYS	Solid linear	0.1mm	350	702	410	877
B	I-DEAS	Solid quad.	0.07mm	340	729	450	971
Coefficient of variation				2.0%	2.7%	6.6%	7.2%

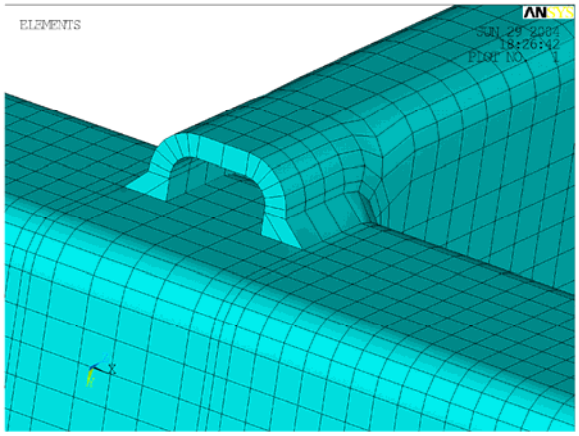

Fig. 5.8: Solid model of participant A (fillet weld without penetration)

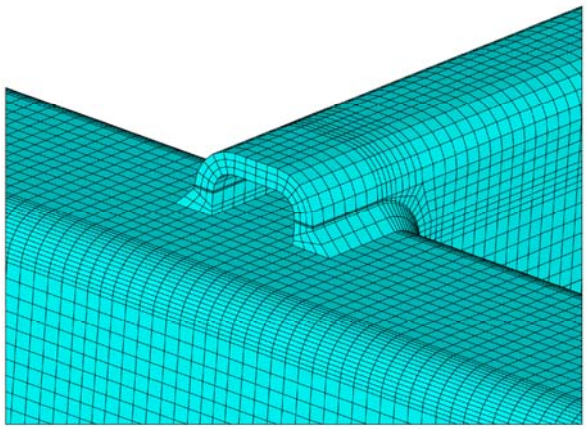

Fig. 5.9: Solid model of participant A (full penetration weld)

The resulting deformations and distribution of principal stresses are shown in Fig. 5.10. At the critical location, both normal and shear stresses act at the weld toe, resulting in changes in the directions of the principal stresses during load cycling, as illustrated in Fig. 5.11. Therefore, the individual stress components had to be extrapolated to the weld toe in this case, based on the recommendations by Niemi et al. (2006). In the case of three elements over the plate thickness, the structural stress was obtained by stress linearization in the plate thickness direction at the weld toe.

The resulting structural hot-spot stresses in Table 5.3 are very similar. However, those for the fillet weld case are significantly higher. This can be explained by changes in local bending due to the increased eccentricity and flexibility of the fillet welded joint.

The effective notch stress was computed by participant A using the sub-model technique and by participant B using a locally refined mesh. The sub-model incorporating the reference radius r_{ref} = 1 mm is shown in Fig. 5.12. The displacements at the boundaries were taken from the overall mesh with three elements in the plate thickness direction (Fig. 5.9). The maximum principal stress in the rounded weld toe was taken as the effective notch stress (Fig. 5.13). Again, the difference between the stresses in the full penetration and fillet welds is relatively large (more than 20%).

5.2.3 Discussion of the results

The variation in the results for both the structural and notch stress analysis is considered to be acceptable in view of the different models and analysis techniques. The type of welding in the actual test specimens (fillet or full penetration) was not clear so both types were analysed; quite different results were obtained. It seems most likely that the joints were made with fillet welds but that some penetration occurred.

The corresponding mean fatigue lives for the two types of weld, based on the fatigue class FAT

225 and a standard deviation of log$N$ = 0.2, were 85,000 and 63,000 cycles. These lives lay either side of the actual mean life from the tests of 75,000 cycles, which is consistent with the actual welds being partial penetration, as suggested above.

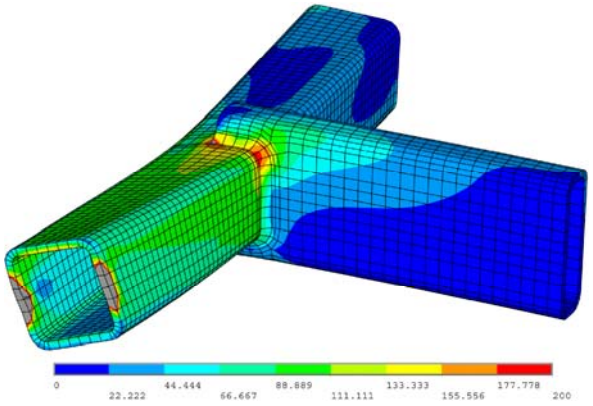

Fig. 5.10: Deformations and principal stresses in the RHS members

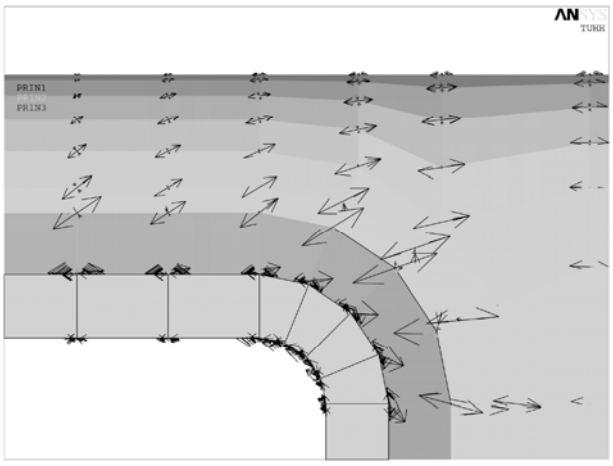

Fig. 5.11: Distribution of principal stresses on the surface of the attached RHS member

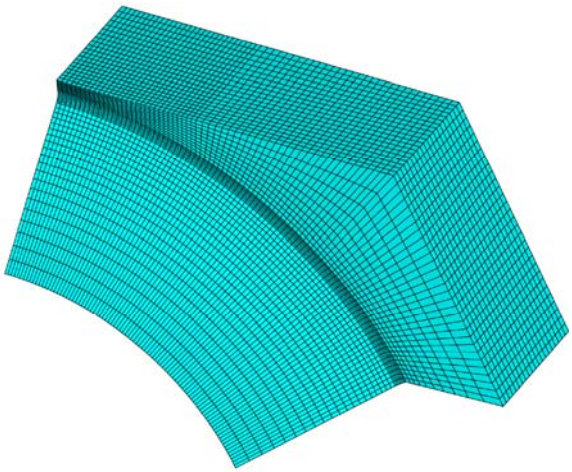

Fig. 5.12: Sub-model of critical area (Participant A)

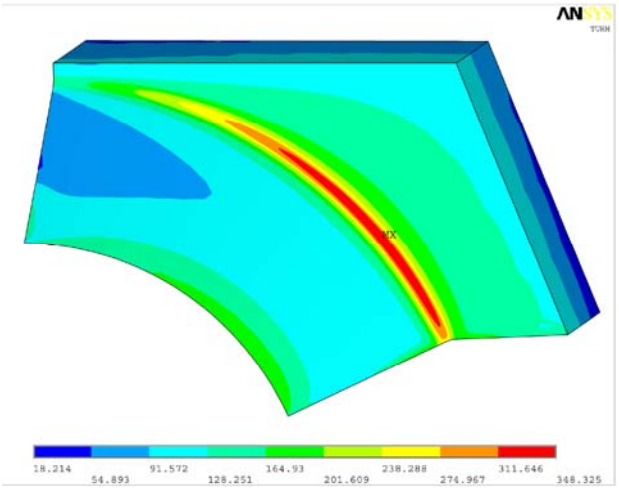

Fig. 5.13: Stress distribution in sub-model (Participant A, full penetration weld)

5.3 Fillet-Welded End Connection of a RHS Member with Non-Fused Weld Root Faces

5.3.1 Description of the detail

The third detail is a fillet-welded connection between two rectangular hollow section (RHS) members, see Fig. 5.14. The dimensions of the RHS were 120 mm x 80 mm x 6 mm (height x width x thickness). The two hollow sections were connected to a 15mm thick intermediate plate using a single-sided fillet weld. The nominal throat thickness *a* of the weld was 4.5 mm. The gap between the intermediate plate and the hollow section was assumed to be zero, see “DET A” in Fig. 5.14.

The two load cases investigated are shown in Fig. 5.15, together with the boundary conditions. In the stress analysis, the left end was fixed according to the symmetry conditions. In the tensile load case, a uniaxial constant stress of 100 MPa was applied to the right end. In the bending load case a distributed shear force of 17.25 N was applied to the right end creating the nominal bending stress of 100 MPa.

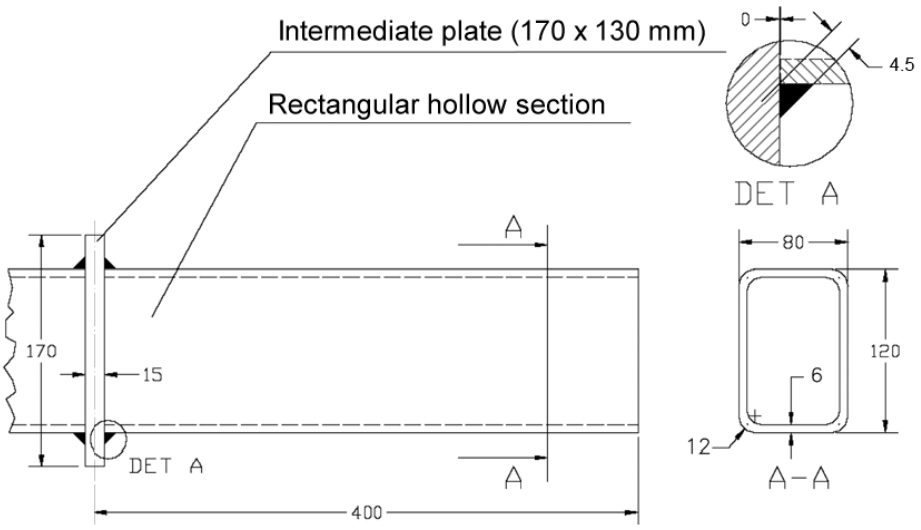

Fig. 5.14: Sketch of the fillet-welded end connection of an RHS member

Specimens of this type were fatigue tested either in tension or bending. Fatigue cracks generally started at the weld root in both cases (Fricke and Kahl, 2006). Under tensile load, fatigue cracks first appeared on the long side of the RHS, while under bending load the first crack appeared on the upper short side, where the bending stress was highest..

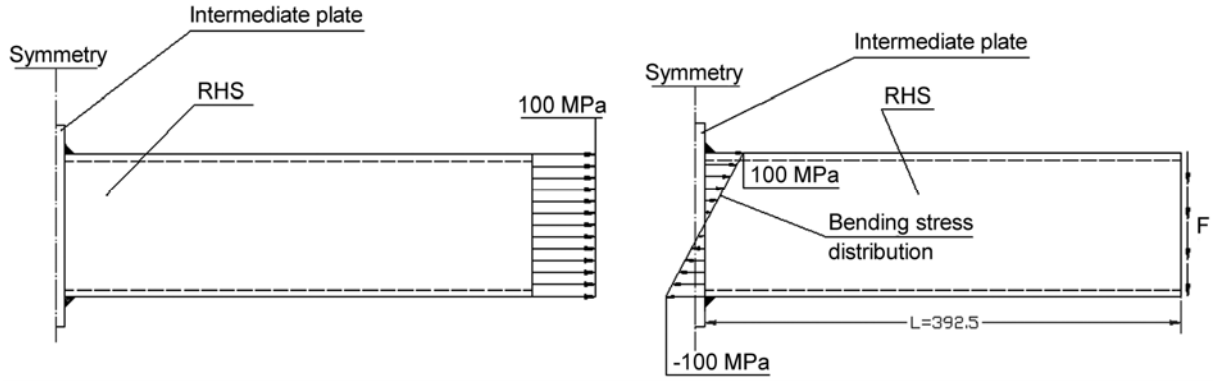

Fig. 5.15: Boundary conditions for tensile (left) and bending loads (right)

5.3.2 Description of the models and analyses results

In total seven models were analysed. In addition to members of the IIW work group mentioned, two participants of the 'Network of Excellence on Marine Structures', which is funded by the European Commission, joined the round robin.

All participants applied the FE method and modelled the structure with solid elements, using the keyhole shape notch for the weld root and taking the theoretical root location as the outer point of the circle with reference radius $r_{ref.}$= 1 mm. Participant A used the sub-model technique, while all others used a refined mesh in the overall model. Symmetry conditions were partly utilised. Table 5.4 gives an overview of the models and the resulting notch stresses (principal stresses).

Figs. 5.16 to 5.19 show some examples of the models used. In most cases, the elements around the keyhole notch were rather small. The longest elements in the circumferential direction, as chosen by participant E (see Fig. 5.17), showed an anomalous distribution of nodal stresses (Fig. 5.18).

Table 5.4: Analysis results for the fillet-welded RHS joint (for nominal stress of 100 MPa)

Partici tici-pant	Program	Element Type (Displace-ment function and shape)	Element length along circumference	Max. notch stress [MPa]	
				Tensile LC	Bending LC
A	ANSYS	quadratic (hexahedral)	~ 0.1 mm	888	637
B	ANSYS	quadratic (hexahedral)	~ 0.25 mm	867	601
C	ANSYS	quadratic (tetrahedral)	~ 0.4 mm	913	650
D	ANSYS	quadratic	Not reported	907	642
E	I-DEAS	quadratic (hexahedral)	~ 0.45 mm	914	644
F	ANSYS	quadratic (tetrahedral)	~ 0.2 mm	864	620
G	ANSYS	quadratic (tetrahedral)	~ 0.3 mm	700	600
Coefficient of variation (all results)				8.7%	3.3%
Coefficient of variation (all results without G)				2.5%	2.9%

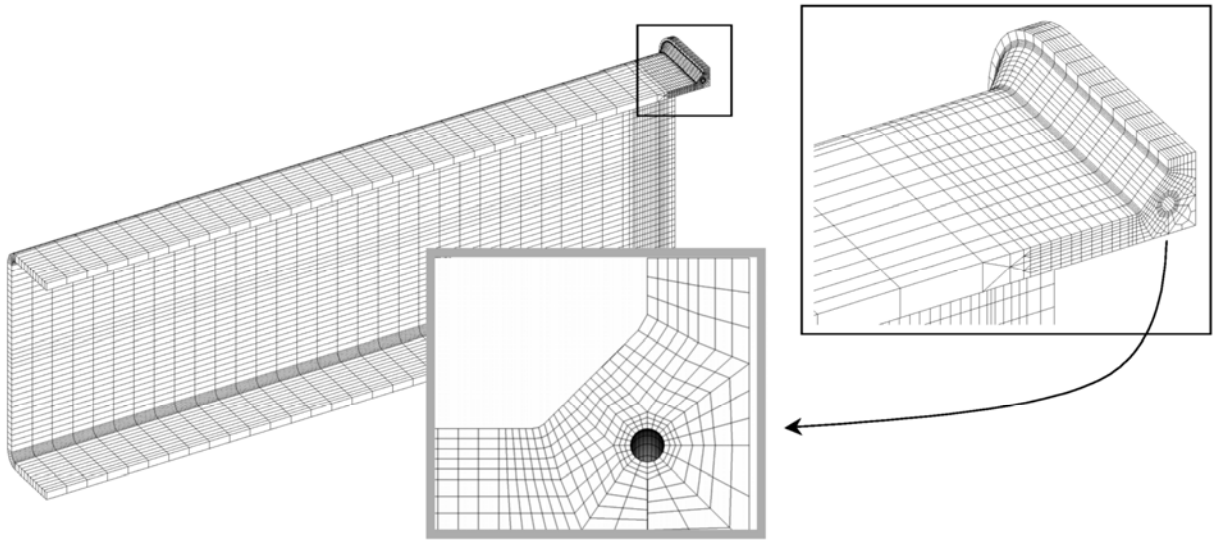

Fig. 5.16: Finite element model of Participant B

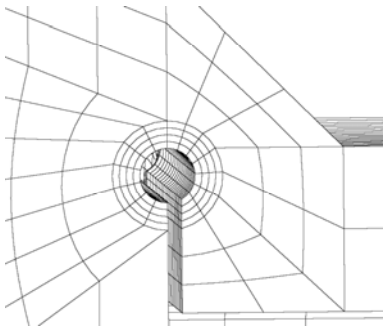

Fig. 5.17: Local mesh of Participant E

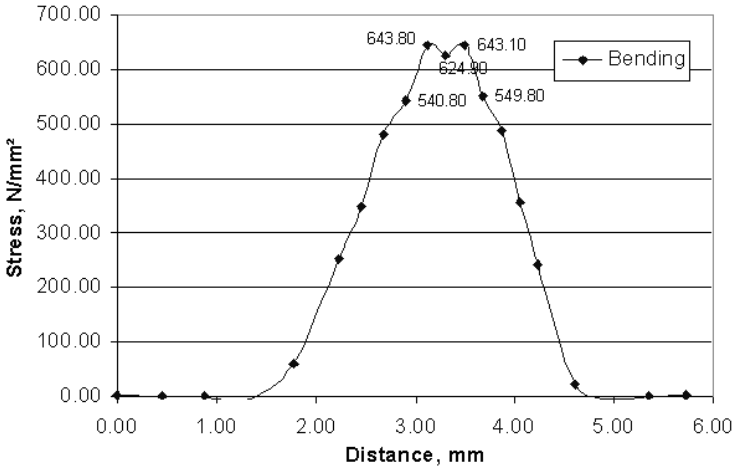

Fig 5.18: Distribution of nodal stresses along circumference (clockwise) for bending load case (Participant E)

The model in Fig. 5.19 is of particular interest. The number of elements around the notch radius was quite high and the element length normal to the surface seems to be appropriate for modelling the steep stress gradient. However, near the most highly stressed plane of the weld, highlighted in the figure, very large elements were used close to the notch surface (indicated by an arrow). Also the element length along the weld line seems to be too large. Such large elements were not able to model the high stress increase in the highlighted plane, resulting in smaller notch stresses compared to all other results.

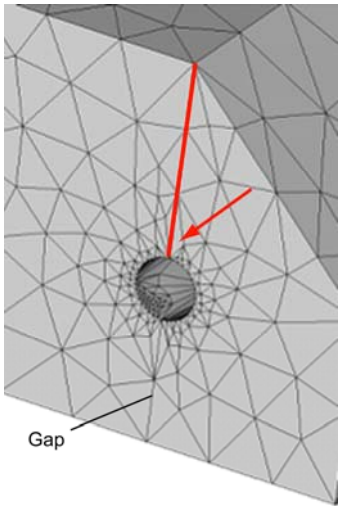

Fig. 5.19: Local mesh of Participant G

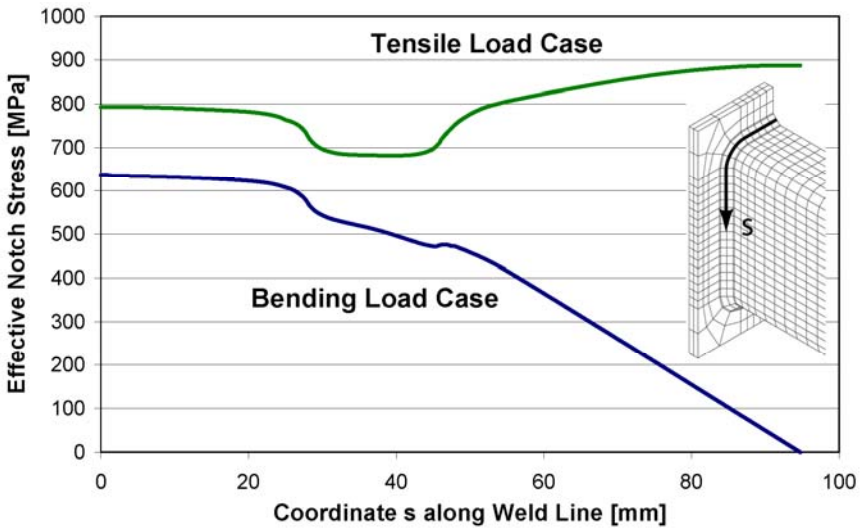

Fig. 5.20: Distribution of the notch stress along the weld root line (Participant A)

In agreement with the failures observed in the tests carried out in tension, the highest notch stress occurred halfway up the long side of the RHS, where more local bending is observed in the weld throat than along the short sides which are more restrained by the corners, see Fig. 5.21. In the bending load case, the highest notch stress occurred in the middle of the upper weld where the largest bending stresses act.

Another interesting aspect was observed in connection with the sub-model technique used by participant A (Fig. 5.21). Initially, a rather coarse overall finite element model of the RHS member was chosen, with only one element in the thickness direction of the wall and the fillet weld. However, the notch stresses obtained from the sub-models were obviously too small. The reason was that the local bending of the weld shown in Fig. 5.22 was different from that in the coarse overall model, which was too stiff, yielding smaller boundary displacements for the sub-model. Therefore, the overall model had to be refined by modelling the weld throat with at least two elements along the weld throat section. This resulted in almost 10% higher stresses, as given in Table 5.4.

5.3.4 Discussion of the results

Although different modelling techniques were used, variations in the results were fairly small if those of participant G are excluded due to the influence of elements that were too large. Another finding, already mentioned, is that the choice of sub-modelling technique is a source of inaccuracy. To achieve reliable results, the sub-model and the respective part of the overall model need to have the same stiffness, as already mentioned in Section 3.

Fatigue lives obtained from fatigue tests of the joint (Fricke and Kahl, 2006) were above the FAT 225 S-N curve when plotted in terms of the notch stress.

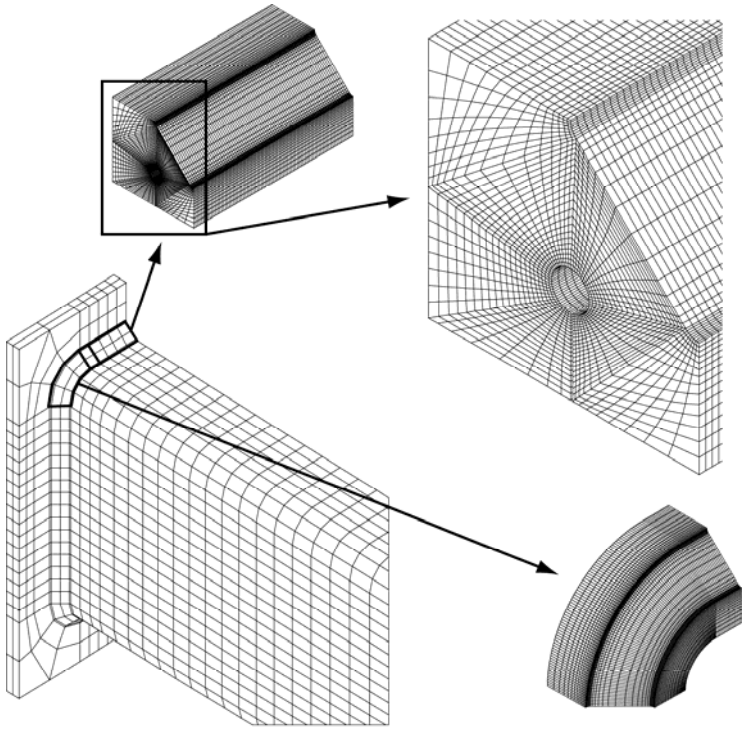

Fig. 5.21: Overall model and sub-models of Participant A

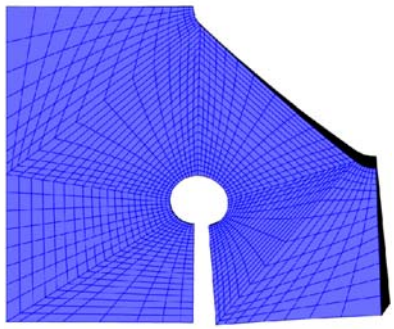

Fig. 5.22: Deformation of the sub-model for bending load

5.4 Spot-Welds in an Automobile Door

5.4.1 Description of the structure

The fourth example is taken from the automotive industry where thin sheets with thicknesses between 0.6 and 3 mm are used. Spot-welding is frequently applied, laser welding not yet to the same extent.

The durability of lightweight structures is of high interest. A typical example is the assessment of the durability of joint techniques in automotive doors and lids, as presented by de Bruyne and Hoppe (2006). Fig. 5.23 shows a spot welded door which is dynamically loaded during closing at a speed of 1.5 m/s.

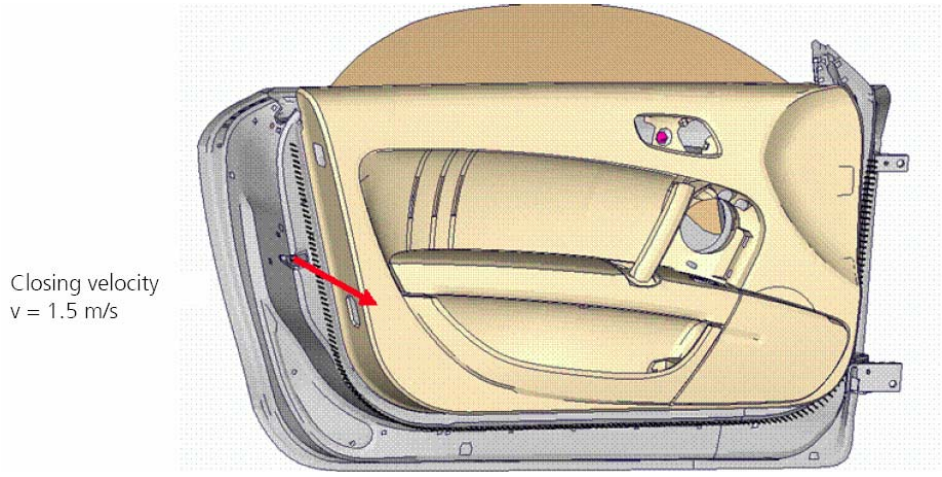

Fig. 5.23: Illustration of the automobile door without the inner frame (de Bruyne and Hoppe, 2006)

The example is selected to show the main procedural steps without judging the quality of modelling which would require a deeper insight into several details. Generally it can be stated that weld spot modelling for strength and stiffness assessment as well as structural optimisation is a highly developed procedure in automotive engineering, see also Radaj et a. (2006, ibis pp. 373-376 and 427-429).

5.4.2 Description of the model

Because of the relatively thin material, the small-size notch approach has been applied.

The spot-welds were analysed using super-elements, as shown in Fig. 5.24, being gradually refined at the root notch. It should be noted that the mesh is somewhat coarser than recommended in Table 3.1. The connection to the overall finite element model made from shell elements was provided by 8 nodes at the four corners of each sheet, having six degrees of freedom. Special coupling elements along the boundaries are used to improve the compatibility of the displacements with those of the overall model. The technique allows the analysis of large spot-welded structures. The topology of the super-element is independent of the sheet-thickness. The parametric super-element is automatically adapted to the actual geometry of the spot-weld and the plate thicknesses.

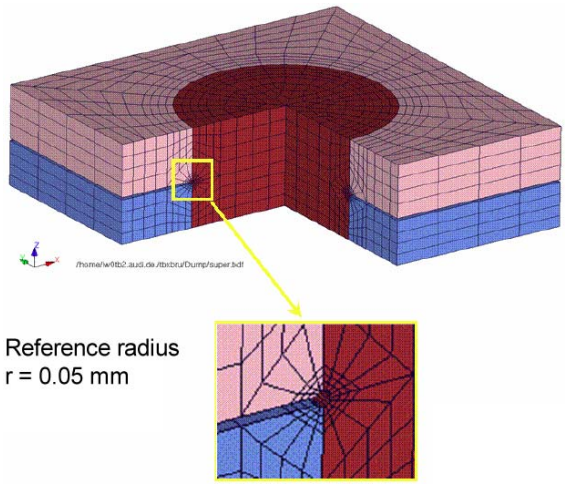

Fig. 5.24: Super-element of a spot-weld with reference radius r_{ref} = 0.05 mm (de Bruyne and Hoppe, 2006)

5.4.3 Fatigue assessment

The fatigue assessment was based on the mean S-N curve derived from fatigue tests of simple specimens.

The variation in the maximum principal stress in the notch of a selected spot-weld for one door closing (left part of Fig. 5.25) shows one large pulsating tension cycle, and this is taken to estimate the fatigue life (right part of Fig. 5.25), resulting in this case in 4,000 cycles.

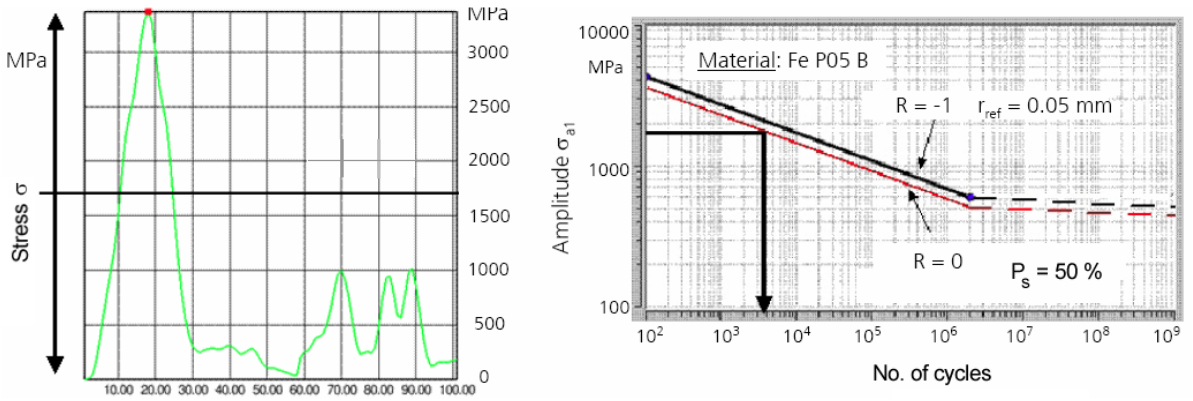

Fig. 5.25: Variation in the maximum principal notch stress and estimated fatigue life (de Bruyne and Hoppe, 2006)

Fig. 5.26 displays details of the calculation model, the location of the critical spot-weld and an example of a fatigue test specimen that showed cracks after 10,000 cycles. Both the critical location and the fatigue life obtained from the calculation agreed quite well with the experimental findings.

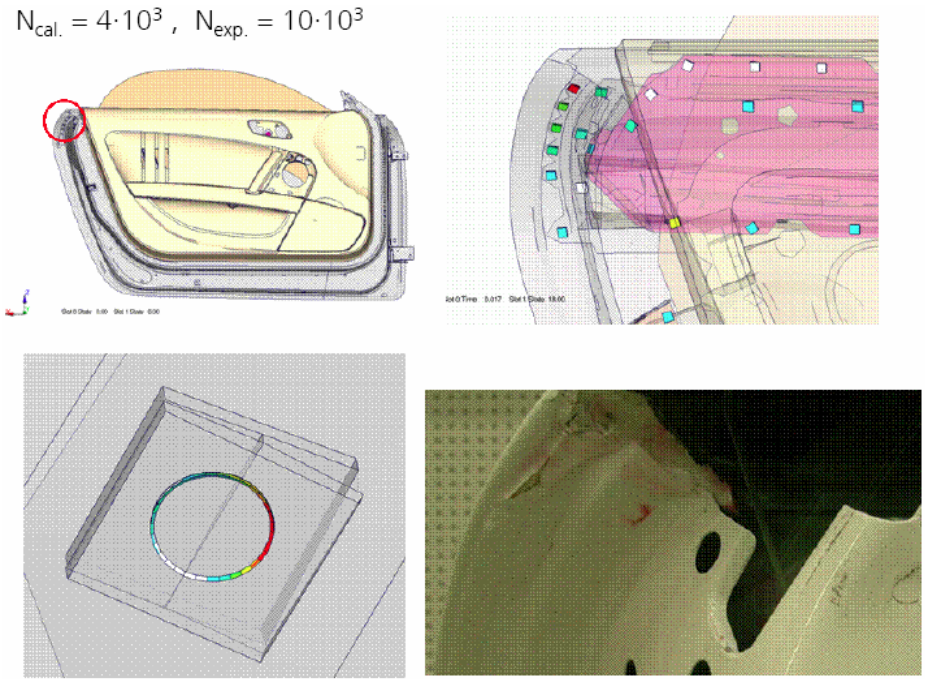

Fig. 5.26: Details of the calculation model and a fatigue test specimen (de Bruyne and Hoppe, 2006)

6. Acknowledgement

The document is a product of several years of study by Working Group 3, 'Stress analysis' of IIW Commission XIII. The Support by the Chairmen of Commission XIII, Prof. S.J. Maddox (UK) and later Prof. G. Marquis (Finland), and of the Joint Working Group of IIW Commissions XIII/XV, Prof. A. Hobbacher (Germany) is appreciated. Special acknowledgement is made to Prof. D. Radaj, Prof. T. Seeger and Prof. C.M. Sonsino (Germany) as well as to Prof. J. Samuelsson and his co-workers (Sweden) for their contributions, support and critical reviews. Also the participants of the IIW round-robin including the contributors of the MARSTRUCT Network of Excellence, coming from several countries (see Fricke, 2006), are thanked for their numerical analyses and comments. F. de Bruyne and A. Hoppe are thanked for providing the automotive example.

7. References

Anthes R J, Köttgen V B and Seeger T (1993): Kerbformzahlen von Stumpfstößen und Doppel-T-Stößen. *Schweißen und Schneiden* 45(12), 685-688.

Banerjee P K (1994): *The Boundary Element Methods in Engineering*. McGraw-Hill, New York.

Bathe, K J (1996): *Finite Element Procedures*. Prentice Hall, Englewood Cliffs (2nd Ed.).

Brebbia C A, Telles J C and Wrobel L C (1984): *Boundary Element Techniques*. Berlin: Springer-Verlag.

Brennan F P, Peleties P and Hellier A K (2000): Predicting weld toe stress concentration factors for T and skewed T-joint plate connections. *Int. J. Fatigue*, 22(7), 573-584.

de Bruyne F and Hoppe A (2006): Virtual durability assessment for joint techniques in automotive doors and lids (in German). Proc. 13th Int. Kongress Berechnung und Simulation im Fahrzeugbau., VDI-Wissensforum Düsseldorf.

Cook R D, Malkus D S, Plesha M E and Witt R J (2002): *Concepts and Applications of Finite Element Analysis*. John Wiley, New York (4th Ed.)

Cruse T A (1988): *Boundary Element Analysis in Computational Fracture Mechanics.* Dordrecht: Kluwer Academic.

Eibl M; Sonsino CM; Kaufmann H and Zhang G (2003): Fatigue Assessment of Laser Welded Thin Sheet Aluminium. *Int J Fatigue*, 25, 719–731

Fricke W (2006): Round-Robin Study on Stress Analysis for the Effective Notch Stress Approach. *Welding in the World* 51, No. 3/4, 68-79

Fricke W and Kahl A (2006): Fatigue assessment of weld root failure of hollow section joints by structural and notch stress approaches. *Proc. of Int. Symp. on Tubular Structures* (ISTS'11), Quebec.

Fricke W and Kahl A (2007): Local stress analysis of welded ship structural details under consideration of the real weld profile. *Proc. Int. Symp. on Practical Design of Ships and Floating Structures*, Houston.

Fricke W, Paetzold H and Zipfel B (2008): Fatigue Life Investigation of a Connection of Steel Sandwich Plates. Doc. XIII-2244r1-08, International Institute of Welding.

Gaul L, Kögl M and Wagner M (2003): *Boundary Element Methods for Engineers and Scientists*. Springer-Verlag, Berlin.

Gosch T and Petershagen H (1997): Effect of undercuts of the fatigue strength of butt joints (in German). Schweißen & Schneiden 49(3), 158-163.

Hobbacher A (1996): *Fatigue Design of Welded Joints and Components*. Abington Publ., Cambridge.

Hobbacher A (2007): Recommendations for Fatigue Design of Welded Joints and Components, Final Draft. IIW-Doc. XIII-2151r1-07 / XV-1254r1-07, International Institute of Welding.

Hobbacher A (2008): Database for the Effective Notch Stress Method at Steel. IIW Joint Working Group Doc. JWG-XIII-XV-197-08, International Institute of Welding

Hughes T R (1987): *The Finite Element Method - Linear Static and Dynamic Finite Element Analysis*. Prentice Hall, Englewood Cliffs.

Iida K and Uemura T (1995): Stress concentration factor formulas widely used in Japan. *Fatigue and Fracture in Engng. Materials and Structures*, 19 (6), 779-786, and IIW Doc XIII-1530-94.

Karakas Ö; Morgenstern C; Sonsino C M; Hanselka H; Vogt M; Dilger K (2007): Grundlagen für die praktische Anwendung des Kerbspannungskonzeptes zur Schwingfestigkeitsbewertung von geschweißten Bauteilen aus Magnesiumknetlegierungen. LBF-Report FB-232, Fraunhofer-Inst.

für Betriebsfestigkeit & Systemzuverlässigkeit, Darmstadt and ifs-Report 17, Inst. für Schweißtech. Fertigungsverfahren der TU Braunschweig, Braunschweig.

Köttgen R, Olivier R and Seeger T (1991): Schwingfestigkeitsanalyse für Schweißverbindungen auf die Grundlage örtlicher Beanspruchungen (Fatigue analysis of welded connections based on local stresses). *Expert '91 – Berechnung, Gestaltung und Fertigung von Schweißkonstruktionen im Zeitalter der Expertensysteme*, DVS-Bericht 133, 75-85, Düsseldorf, DVS, 1991, and IIW Doc XIII-1408-91.

Kuguel R (1961): A relation between theoretical stress concentration factor and fatigue notch factor deduced from the concept of highly stressed volume. *ASTM Proc 61*, 732-744.

Kyuba, H. and Dong, P. (2003): Equilibrium-equivalent structural stress approach to fatigue analysis of a tubular joint. IIW-Doc. XIII-1992-03/XV-1149-03, Int. Inst. of Welding.

Lawrence F V, Ho N J and Mazumdar P K (1981): Predicting the fatigue resistance of welds. Ann. Rev. Material Science, Vol. 11, 401-425.

Lehrke H-P (1999): Berechnung von Formzahlen für Schweißverbindungen. *Konstruktion* 51:1/2, 47-52

Lieurade H-P, Huther I und Lebaillif D (2003): Weld quality assessment as regard to Fatigue. *Proc. of the IIW Fatigue Seminar 2003*, Rep. 14, Lappeenranta University of Technology, Finland.

Morgenstern C, Sonsino C M, Hobbacher A and Sorbo F (2004): Fatigue design of aluminium welded joints by the local stress concept with the fictitious notch radius of r_f = 1 mm. IIW Doc XIII-2009-04 and Int. J. Fatigue 28 (2006), pp. 881-890

Neuber H (1946): *Theory of Notch Stresses*, Ann Arbor Mi, Edwards.

Neuber H (1968): Über die Berücksichtigung der Spannungskonzentration bei Festigkeitsberechnungen. *Konstruktion*, **20** (7), 245-251.

Niemi E, Fricke W and Maddox S (2006): *Fatigue analysis of welded joints - Designer's guide to the structural hot-spot stress approach*. Cambridge, Woodhead Publ.

Olivier R, Köttgen V B and Seeger T (1989): Schweißverbindung I (Welded Joints I), FKM-Forschungshefte 143, Frankfurt/M, FKM.

Olivier R, Köttgen V B and Seeger T (1994): Schweißverbindung II, Schwingfestigkeitsnachweise (Welded Joints II, Fatigue Assessments), FKM-Forschungsheft 180, Frankfurt/M, FKM.

Peterson R E (1959): Relation between stress analysis and fatigue of metals', *Proc SESA*, **11** (2), 199-206

Radaj D (1990): *Design and Analysis of Fatigue Resistant Welded Structures*, Cambridge, Abington Publ, 1990.

Radaj D and Zhang S (1991): Multiparameter design optimisation in respect of stress concentration. *Engineering Optimisation in Design Processes*, Berlin: Springer-Verlag, 181-189.

Radaj D, Sonsino C M and Fricke W (2006): *Fatigue Assessment of Welded Joints by Local Approaches*. Abington: Woodhead Publishing (2nd Edition)

Radaj D, Sonsino C M and Fricke W (2008): Recent developments in local concepts of fatigue assessment of welded joints. Submitted to *Int J Fatigue*.

Rainer G (1983): Parameterstudien mit finiten Elementen, Berechnung der Bauteilfestigkeit von Schweißverbindungen unter äußeren Beanspruchungen. *Konstruktion* **37** (2), 45-52

SAE (2003): www.fatigue.org/weld/challenge-1

Siebel E and Stieler M (1955): Ungleichförmige Spannungsverteilung bei schwingender Beanspruchung. *VDI-Zeitschrift*, **97** (5), 121-126

Sonsino C M (1993): Zur Bewertung des Schwingfestigkeitsverhaltens von Bauteilen mit Hilfe örtlicher Beanspruchungen. *Konstruktion* 45/1, 25-33.

Sonsino C M (1995): Multiaxial fatigue of welded joints under in-phase and out-of-phase local strains and stresses. *Int. J. Fatigue* 17, 55-70.

Sonsino C M (2008): Suggested allowable equivalent stresses for fatigue design of welded joints according to the notch stress approach with reference radii r_{ref} = 1.00 and 0.05 mm. IIW Doc. XIII-2216-08/XV-1285-08, International Institute of Welding.

Sonsino, C M and Fricke, W (2006): Some remarks for improving the assessment of multiaxial stress states and multiaxial sprectrum loading in the IIW fatigue design recommendations. IIW Doc. XIII-2128-06/XV-1222-06, International Institute of Welding

Sonsino C M, Radaj D, Brandt U and Lehrke H P (1999): Fatigue assessment of welded joints in AlMg4.5Mn (5083) aluminium alloy by local approaches. *Int J Fatigue*, **21** (9), 985-999, and IIW Doc XIII-1717-98

Sonsino C M and Wiebesik J (2007): Assessment of multiaxial spectrum loading of welded steel and aluminium joints by modified equivalent stress. IIW-Doc. XIII-2158r1-07/XV-1250r1-07, International Institute of Welding

Tsuji I (1990): Estimation of stress concentration factors at weld toe of non-load carrying fillet welded joints (in Japanese). West Japan Soc. of Naval Arch., 80, 241-251.

Zienkiewicz O C und Taylor R L (2000): *The Finite Element Method, Vol. I: The Basis*. Oxford, Butterworth-Heinemann.